IMPLEMENTATION OF A CELL BALANCING SYSTEMS FOR LITHIUM BATTERIES WITH MULTI-LEVEL MONITORING

Jacky Wong Chew Soon

A project report submitted in partial fulfilment of the requirements for the award of Bachelor of Electrical and Electronnic Engineering with Honours

Lee Kong Chian Faculty of Engineering and Science
Universiti Tunku Abdul Rahman

May 2024

DECLARATION

I hereby declare that this project report is based on my original work except for citations and quotations which have been duly acknowledged. I also declare that it has not been previously and concurrently submitted for any other degree or award at UTAR or other institutions.

Signature : Jacky

Name : Jacky Wong Chew Soon

ID No. : 1902238

Date : 16-5-2024

APPROVAL FOR SUBMISSION

I certify that this project report entitled **"IMPLEMENTATION OF A CELL BALANCING SYSTEMS FOR LITHIUM BATTERIES WITH MULTI LEVEL MONITORING"** was prepared by **JACKY WONG CHEW SOON** has met the required standard for submission in partial fulfilment of the requirements for the award of Bachelor of Electrical and Electronic Engineering with Honours at Universiti Tunku Abdul Rahman.

Approved by,

Signature : 

Supervisor : Dr Chew Kuew Wai

Date : 16/5/2024

Signature : 

Co-Supervisor : Dr Hau Lee Cheun

Date : 16/5/2024

ABSTRACT

As technology advances, the demand for batteries, especially in electric vehicles (EVs), continues to grow. Batteries are frequently combined in series and parallel configurations to reach specific voltage and storage capacity requirements. However, maintaining a balanced state of charge (SoC) across all batteries is crucial for efficient operation during steady state, charging, or discharging. This is typically managed by a battery management system, which monitors various parameters to ensure efficient operation. This project focuses on designing a capacitor-switching active balancer and a monitoring system for lithium iron phosphate batteries, monitoring parameters at different levels, from cell to module to system. The experimental results showed that with the implementation of the cell balancing system, the battery performance is significantly extended by ensuring a balanced SoC across all cells. This led to improved efficiency and longer battery life. The real-time monitoring system provided crucial data on voltage, current, and temperature, enabling optimization of the battery system. This integrated approach demonstrates the system's effectiveness in enhancing lithium iron phosphate battery performance, especially in electric vehicles.

TABLE OF CONTENTS

LIST OF TABLES

LIST OF FIGURES

LIST OF SYMBOLS / ABBREVIATIONS

EV	Electric vehicle
BMS	Battery management system
SoC	State of Charge
LIBs	Lithium-ion batteries
LiFePO4	Lithium Iron Phospate
CC	Coulomb counting
KF	Kalman filter

LIST OF APPENDICES

CHAPTER 1

INTRODUCTION

1.1 General Introduction

With the continuous evolution of technology, the increasing demand for batteries has become an essential factor in modern applications as primary power sources. These applications comprise not only laptop computers and smartphone, but also electric vehicles (EVs), power grid storage system, and other high-power demanded devices that run on batteries. A device with minimal power requirements, such as a cell phone or portable device, could get by with just one battery cell. However, numerous battery cells are needed for applications like mobile devices, high-performance machinery like electric vehicles, and tasks like load balancing. The lithium-ion battery has steadily gained popularity compared to the nickel and lead-acid battery as the most common form of battery in recent years (Bashir et al., 2022). The primary reason for this trend is due to its exceptional characteristics, which include significant capacity, increased charge/discharge rates (C-rate), and the absence of memory effects (Paidi and Gudey, 2022).

In applications like EV and grid energy storage, batteries are typically arranged in series and parallel configurations to meet the required voltage and capacity specifications. In layman's term, a battery pack is created by combining a specific number of battery modules with various control and protective systems. When it comes to EVs, it is crucial to know that the terms battery and battery pack are interchangeable. However, when batteries are connected in series, some sort of circuitry are required to balance each individual cell. When each battery is manufactured at the factory, it comes with a unique profile containing battery parameters like nominal capacity, open circuit voltage, internal impedance, etc. Any deviations in these parameters will undoubtedly result in the deterioration of the overall system performance, and in severe cases, even lead to battery module failure. As a result, they are typically cotnrolled by a battery management system that

monitors their parameters and ensures their efficient operation (Pelin et al., 2022).

1.2 Importance of the Study

The primary focus of this project revolves around the investigation of cell balancing techniques and the implementation of a monitoring system capable of assessing battery parameters at the cell, module, and system levels. Numerous concerns can arise if there are substantial variations in any of the battery parameters includes thermal runaway caused by overcharging, overheating, and high temperatures, cell cycle degradation or uneven aging, and a decline in the overall system efficiency. Among this issues thermal runaway is the most crucial as the combustible electrolytes can contribute to a fire that is extremely difficult to control (Pelin et al., 2022).

To assess whether the cell is being balanced in terms of charging and discharging, the battery's state of charge (SoC) will be evaluated using various techniques including voltage estimation, coulomb counting, and temperature measurement. However, the study of SoC estimation methods should be continued, as these methods still cannot provide accurate results for determining battery capacity. The amount of electricity that can be drawn from a series battery arrangement is constrained by the battery with the least capacity. The highest capacity battery is susceptible to being overcharged during the charging process, potentially resulting in excessive heat generation and even an explosion (Li et al., 2023). Addressing these concerns through sophiscated monitoring and balancing methods paves the way for improved battery performance, extended battery life cycle, and lower safety threats. This initiative will ultimately help to enhance and sustain energy storage technologies.

1.3 Problem Statement

Optimizing battery performance and safety is a crucial challenge for energy storage devices. The issue stems from variances in capacity and state of charge (SoC) among individual cells inside battery packs. These imbalances can have serious impacts such as thermal runaway, uneven aging, and decreased overall

system efficiency. The lack of precise real-time monitoring deteriorate these issues, delaying their ability to immediate identify and resolve. As a result, developing comprehensive solutions to rectify these imbalances and assure the safe operation of energy storage systems is critical.

While various external sources have investigated cell balancing approaches and monitoring systems, questions about their real usefulness in achieving successful cell balancing remain. Furthermore, inaccurate in estimating the battery SoC lead to faster rate of cell degradation and efficiency of the energy storage system, impacting their economic and environmental sustainability. Hence, it is important to pave the path for improved energy storage options by digging into the study and invention of cell balancing and monitoring which will be implemented in this project. These technologies not only increase battery life and improve system efficiency, but they also help to make renewable energy integration and electric vehicle propulsion systems safer, more reliable, and environmentally sustainable.

1.4 Aim and Objectives

The aim of this study is to develop a comprehensive monitoring system capable of monitoring cell unbalance during steady state, charging and discharging processes, spanning from the cell level to the module level and ultimately to the system level. This monitoring system will provide relevant feedback to a control system, enabling it to effectively balance the cells.

The objectives of this study are as follows:

1. Develop a monitoring system capable of observing various parameters such as battery voltage, current and temperature at the cell, module and system levels.
2. Design and implement capacitor-based active balancing system for lithium batteries capable of balancing battery voltages at different levels.
3. Evaluate the performance of the cell balancing system and monitoring systems in terms of efficiency, accuracy, and reliability under different operating conditions.

1.5 Scope and Limitation of the Study

The monitored battery system comprises cell-level, module-level, and system-level components. To streamline the functionality of both the battery monitoring system and the cell balancing circuit, a module will be created which consists of 4 batteries in series. Subsequently, two of these modules will be combined at the system level. The battery type used is lithium iron phosphate, which is commonly used in electric vehicles. The primary objective of this designed system is to identify the monitoring system's capability to assess the status of each individual battery, while also ensuring that the cell balancing circuit can appropriately respond to equalize the SoC across all cells.

The findings of this project may solely be applicable to lithium iron phosphate batteries and may not be directly transferrable to other battery chemistries, such as nickel-cadmium batteries or lead-acid batteries. Besides, the results could potentially be confined to the specific battery configuration chosen for this study, namely four batteries in series as a module and two sets of them in parallel as a system. As a result, the extrapolation of these findings to larger battery systems could be compromised. The study also assume idealized condition and does not account for external influences such as user behaviour, charging patterns, and the testing environment which can significantly impact battery performance. The study also may not extensively address safety measures related to the monitoring and balancing, which are one the most important aspects in battery management system.

In addition, the main parameters to be observed for the battery in the monitoring system are voltage, current, and temperature. Voltage will be used as the primary indicator for the SoC of the battery. However, this limits the accuracy of SoC estimation since LiFePO4 batteries exhibit a very flat voltage profile across a wide range of SoC. Besides, the analysis of the performance of the cell balancing system and monitoring system in terms of efficiency, accuracy, and reliability under different operating conditions is also limited. This is because more advanced technologies proposed in external sources were not practically implemented and compared in this project. The project focuses solely on the analysis of the proposed and implemented solution within its scope.

1.6 Contribution of the Study

This study makes a significant contribution to the field of lithium battery management systems by testing the currently available cell balancing system as reported in the research literature, with multi-level monitoring capabilities. By integrating real-time monitoring of individual cell voltages, current and temperatures, the system ensures efficient and effective cell balancing, thus improving overall battery performance and lifespan. This advancement addresses a key challenge in battery management systems and enhances battery management practices. The proposed system's potential for industry adoption, particularly in electric vehicles and renewable energy systems, highlights its practical significance. Additionally, this study provides a foundation for future research in optimizing the system for different battery chemistries and applications.

1.7 Outline of the Report

Chapter 1 of this report discusses the project in detail, including the introduction, importance of study, problem statements, aims, objectives, and the scope and limitations of the study. In chapter 2, a comprehensive literature review of the project is conducted. Various battery types are discussed, along with different types of cell balancers which are categorised into passive and active balancer. Besides, methods for estimating the battery’s State of Charge (SoC) are listed for comparison.

Chapter 3 of this report discusses the hardware and software used in this project, providing clear descriptions of each component. A block diagram of the proposed system is also included for illustration purposes. This chapter also details the hardware and software setup, including Node-RED and MATLAB Simulink. Chapter 4 analyzes the collected data, including the charging and discharging profiles of the LiFePO4 battery. It also compares the results between the software and hardware implementations of the proposed balancer in three cases: battery in steady state, charging, or discharging. Finally, Chapter 5 concludes the overall findings of this project and introduces some recommendations and improvements for future work.

CHAPTER 2

LITERATURE REVIEW

2.1 Introduction

In this chapter, various types of batteries, primarily including lead-acid, nickel, and lithium-ion batteries, will be thoroughly reviewed. The review will encompass their evolution, advantages, and disadvantages. Additionally, different cell balancing techniques, which can be broadly categorized into two main branches, passive and active, will be explored with a comprehensive study of the circuit implementation of each technique. Furthermore, the factors that affect battery lifespan, performance, and temperature will be examined in great detail to better understand battery behavior. It it known that one of the critical parameters to monitor in cell balancing techniques is the battery state of charge (SoC). Therefore, different methods of SoC estimation will also be thoroughly discussed in this chapter.

2.2 Battery Type

There are three main types of batteries used in modern applications today: lithium batteries, lead-acid batteries, and nickel-based batteries. The lead-acid rechargeable battery mainly used in specific applications such as vehicle starting, lighting, and ignition. However, it exhibits relatively moderate specific energy and energy density values (approximately 40 Wh kg−1 and 90 Wh L−1). In comparison with advanced lithium-ion batteries, LIBs can offer significanly high energy density value which is around 260 Wh kg−1 and 700 Wh L−1 at the cell level. Following this, the battery industry emerge into the new era with nickel-based technology including nickel-zinc (Ni-Zn) batteries and nickel-metal hydride (Ni-MH) batteries. Both batteris has the advantage of high specific energy and cost-effectiveness and the only trade-off is they have limited cycle life. In the following subsection, each battery type will be comprehensively discussed (Liu et al., 2022).

2.2.1 Lead-Acid Batteries

Being the first commercially successful battery, the lead-acid battery as shown in **Figure 2.1** has maintained dominance in the industry market for over a century due to its cost effectiveness and well-established technology. Specifically, the valve-regulated lead-acid (VRLA) battery has experienced significant advancements concerning specific energy, power delivery, and recharging rate, lead to it particularly suitable for vehicle applications. Furthermore, it exhibits various remarkable advantages such as stable and reliable performance in both high and low temperature, high energy efficiency, and adjustable sizing, Among the promising lead-acid battery type, the bipolar VRLA and UltraBattery stand out compared to others (Liu et al., 2022).

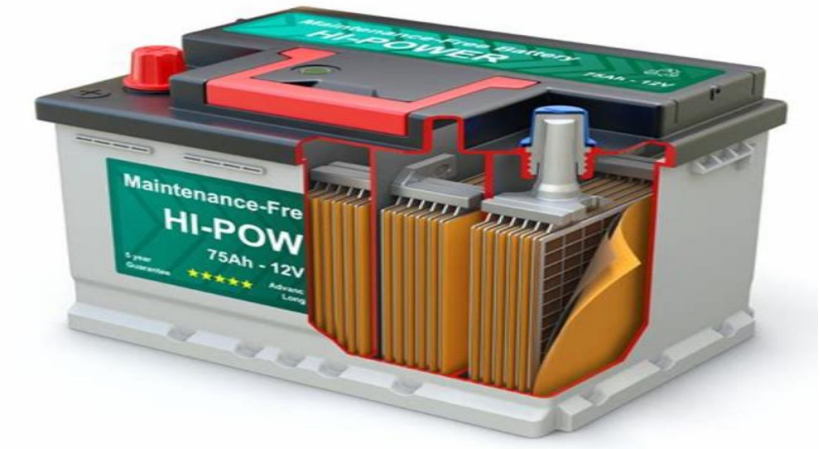

Figure 2.1: External and internal structure of lead-acid battery (Paul, 2021).

2.2.2 Nickel-based Batteries

With the use of nickel oxyhydroxide as the cathode material, a list of nickel battery types has been established. This comprises nickel–iron (Ni–Fe), nickel–cadmium (Ni–Co), nickel–zinc (Ni–Zn), nickel metal hydride (Ni–MH), and nickel–hydrogen (Ni–H2) batteries. Generally, the Ni–Zn battery stands out with a nominal cell voltage of 1.6 V, marking the highest within the nickel-based battery category. It surpasess the Ni-Co battery, offering high specific energy and more environmental friendly due to its non-toxicity properties. Besides, it can tolerate for both overcharging and overcharging, excel in high rate of charge and discharge scenario and maintain efficiency across wide range of temperature range. However, one of its drawback is it exhibit short cycle life of around 300 cycles as the zinc species in its

electrolute is partially soluble. This severely contrains its path to commercialization and as a result, the battery chemistry of Ni-Zn batteries remains an active research focus. Conversely, Ni-MH battery has solidified its position in the EV market since 1992, due to its proven technology and favourable key performance indicators (KPIs). Featuring a nominal cell voltage of 1.32 V, it outperforms lead–acid batteries in terms of specific energy, which lead to their application in certain EV models (Liu et al., 2022). One of the types of nickel-based batteries, known as the nickel-cadmium battery, is depicted in **Figure 2.2**.

Figure 2.2: Nickel-cadmium battery with 1.2V (DKHARDWARE, n.d.).

2.2.3 Lithium-ion Battery

Following the trend of successful commercialization, lithium-ion batteries (LIBs) have became dominant application in electric vehicle (EV) system due to their outstanding advantages such as high energy density, safety and lifespan. A typical LIB cell structure consists three essential components: The anode, cathode, and electrolyte, which also might includes a separator. Efforts in electrochemical innovation primarily focus these components to enhance battery key performance indicators (KPIs). The internal structure of battery is illustrated in **Figure 2.3**. During charging and discharge processes, lithium ion will move between the two electrodes. Beyond the inner workings of the LIB

cell, the external circuit manages the electron flow for power comsumption. To summarize, a high energy density and specific energy battery rely primarily on the material selection and battery design (Liu et al., 2022).

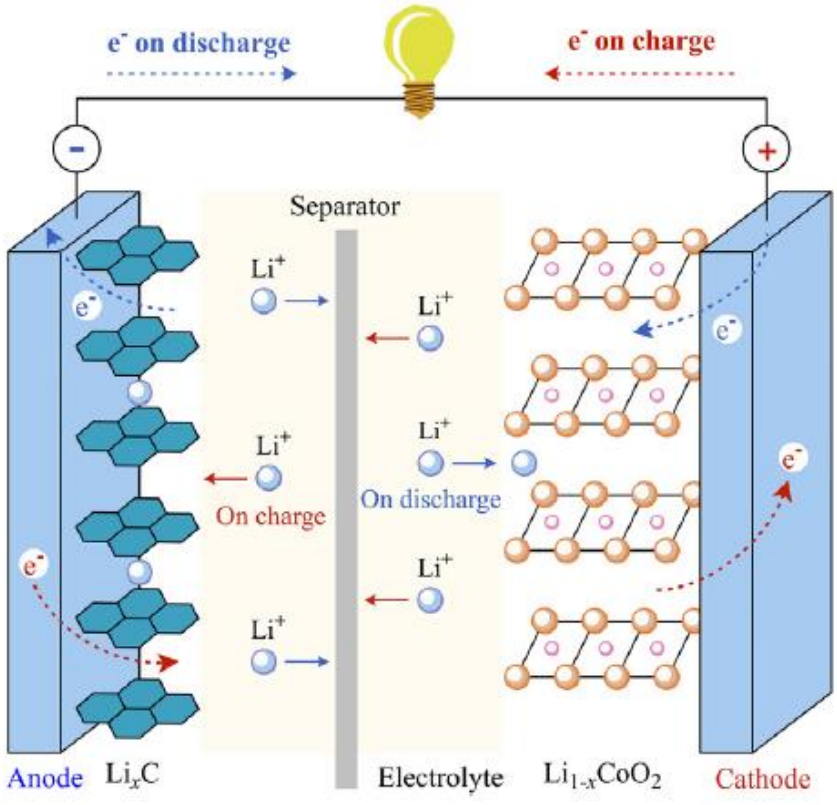

Figure 2.3: Internal structure of lithium-ion battery which consists of anode, cathode, electrolyte and separator (Liu et al., 2022).

In the 1980s, the groundbreaking work of Goodenough and his collaborators marked the inception of a new era for lithium-ion batteries (LIBs) as power sources. **Figure 2.4** emphasizes three key phases of significant advancement in lithium-ion battery (LIB) development—commercialization from 1991, exploration from 2008, and foresight from 2019. The first generation of LIBs utilized LiCoO2 and both the anode and cathode were manufactured with petroleum coke. Subsequent generations brought enhancements in the electrolyte and switching of anode material from hard carbon to graphite, leading to improved energy density. The contemporary cathode materials of choice, such as layered lithium nickel cobalt manganese oxides (Li[NixCoyMnz]O2, abbreviated as NCMxyz), offer higher capacities

and cost reductions compared to LiCoO2 while graphite remains the prevailing anode material (Liu et al., 2022).

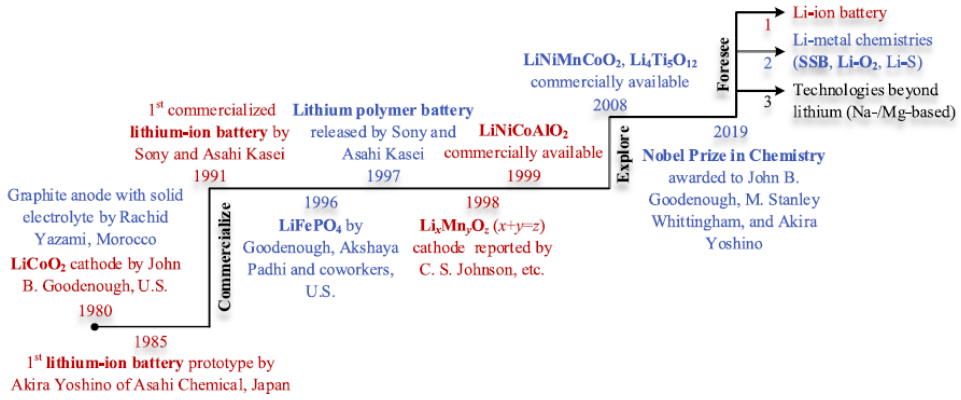

Figure 2.4: Milestones and foresight of lithium battery evolutions (Liu et al., 2022).

Increasing the nickel content in cathode layered oxides to over 80% and incorporating silicon into the graphite negative electrode enhances the energy density and lowers the cost of lithium-ion batteries (LIBs). NCM622 (Li[Ni0.6Co0.2Mn0.2]O2) and NCM811 are emerged as state-of-the-art materials for automotive applications while graphite is the dominant anode material, where a few cells incorporate small amounts of silicon (SiOx). LiMn2O4 (LMO) is occasionally blended with NCM to balance power-to-energy ratios, although high-energy NCM materials are gradually replacing LMO. Despite lower energy density, lithium iron phosphate (LiFePO4 or LFP) cells are gaining popularity in automotive applications due to exceptional safety, extended cycle life, and cost-effectiveness (Liu et al., 2022).

2.3 Passive Balancing Method

Passive balancing method refers to the ultillization of dissipative techniques in balancing cells. In contrast to active balancing circuit, passive balancers are often simpler and more cost effective. The functioning of a passive balancer is relatively straightforward – excess charge is dissipated, as the name implies. Typically, a shunt element is placed across a single cell to release excess charge as heat, while the other cells continue to charge. Each cell within the series string necessitates its own shunt element and these shunt can be

activated simultaneously. The shunt element allows the passing of charger's produced current to prevent overcharging of the cells (Bashir et al., 2022).

Passive cell balancing can be classified into two main types: fixed shunt resistor balancing and switching shunt resistor balancing. In the fixed shunt resistor approach, a constant current flows through all the series-connected cells, and a resistor connected across each cell is adjusted to restrict the cell voltage. This technique is advantageous due to its simplicity and cost-effectiveness. However, it's unsuitable for lithium-ion batteries as it could lead to overcharging in certain instances, potentially causing damage to the cells. **Figure 2.5** outlines the process of fixed cell balancing using flowchart and the circuit configuration (Paidi and Gudey, 2022).

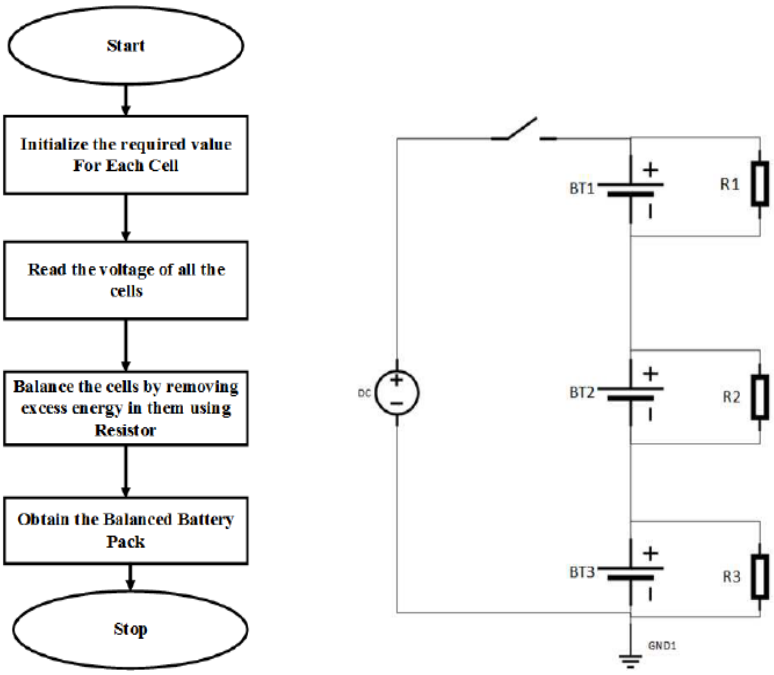

Figure 2.5: Flowchart and schematic diagram of fixed shunt resistor balancing (Paidi and Gudey, 2022).

In the switching shunt resistor technique, the objective is to efficiently extract excess energy from higher cells while maintaining control. This is achieved by utilizing switches that facilitate controlled energy dissipation. This approach offers two distinct operational modes:

- Simultaneous Control Mode: In this mode, all switches are adjusted collectively to manage the energy dissipation from the higher cells.

- Individual Cell Detection Mode: In this alternative mode, the voltage of each individual cell is monitored. This enables the identification of cell voltage imbalances. Subsequently, the switches are selectively operated based on this voltage data, ensuring a more precise energy dissipation process.

Compared to the conventional fixed shunting resistor method, this technique demonstrates greater efficiency. Notably, it finds valuable application in LIBs employed in EV (Paidi and Gudey, 2022). **Figure 2.6** outlines the process of switching shunt cell balancing using flowchart and the circuit configuration.

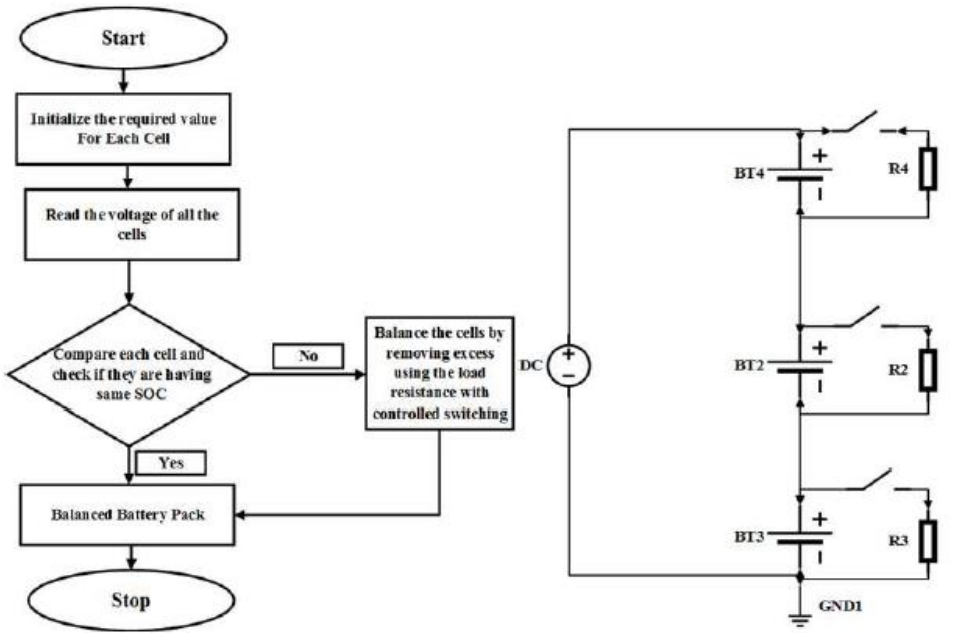

Figure 2.6: Flowchart and schematic diagram of switching shunt resistor balancing (Paidi and Gudey, 2022).

Passive balancing offers a straightforward method to safeguard series-stacked cells from overcharging, potentially at a lower cost compared to more intricate balancing techniques. However, passive balancers dissipate excess energy as heat, resulting in potential heat-related challenges. These balancers

also lack the ability to balance during discharge, making them suitable for scenarios prioritizing initial cost over energy efficiency (Bashir et al., 2022).

2.4 Active Balancing Method

Active balancing techniques involve the utilization of components like capacitors, inductors, transformers, and various prevalent power electronic converter configurations. The objective is to distribute energy among units within a system. This redistribution involves transferring energy from units with higher charge to those with lower charge, thus prevent the energy losses associated with dissipative methods. Active cell balancing offers significant advantages for instance, providing good balancing speed and efficacy. However, this approach includes many components which leads to the increase of cost as well as the complexity of the balancing circuit design (Bashir et al., 2022).

2.4.1 Capacitor Based Cell Balancing

The main component of the capacitor based cell balancing is the capacitor itself. Capacitors play a vital role in achieving equilibrium among cells by facilitating the transfer of energy between adjacent cells. However, there are some drawbacks associated with this approach, including energy dissipation during the charging of capacitors and a subsequent delay in achieving balance. There are many switched capacitors configurations such as single-tiered, double-tiered, and multiple capacitors (Gallardo-Lozano et al., 2014).

The single-tiered switched capacitor based cell balancing topology is shown in **Figure 2.7**. This technique involves a continuous alternation between two distinct states. In the initial state, every capacitor is connected in parallel with its corresponding upper cell. As a result, the capacitor aligns with the voltage of the cell, either supplying or drawing energy from it. Once each capacitor attains the voltage of its corresponding upper cell, the system transitions to the second state (Gallardo-Lozano et al., 2014).

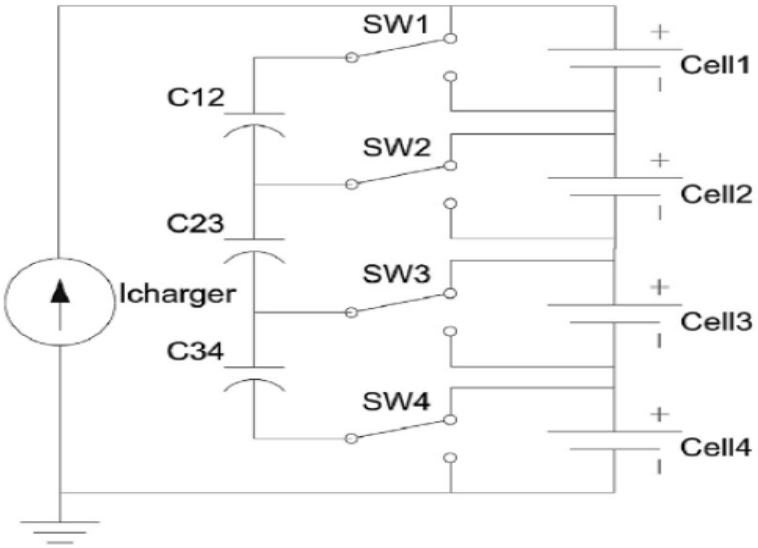

Figure 2.7: Single-tiered switch capacitor method (Gallardo-Lozano et al., 2014).

In the second state, the capacitors are linked in parallel with their corresponding lower cells. This configuration facilitates the transfer or uptake of energy from these cells to achieve a new voltage level. Through repeated cycles of this process, both cells gradually achieve balance. The advantages of this configuration including high efficiency, simplicity, and suitability for both low and high-power scenarios. It eliminates the need for sensing or closed-loop control. However, its primary drawback lies in its speed. The balancing process slows down when the voltage difference between neighboring cells diminishes, resulting in lower balancing currents and subsequently reduced balancing speed (Gallardo-Lozano et al., 2014).

The double-tiered switched capacitor approach is a variation of the single-tiered switched capacitor technique, differing in its utilization of two tiers of capacitors for energy transfer. Generally, this modification reduces equalization time even to a quarter of the original duration (Gallardo-Lozano et al., 2014). The double-tiered switched capacitor topology is shown in **Figure 2.8**.

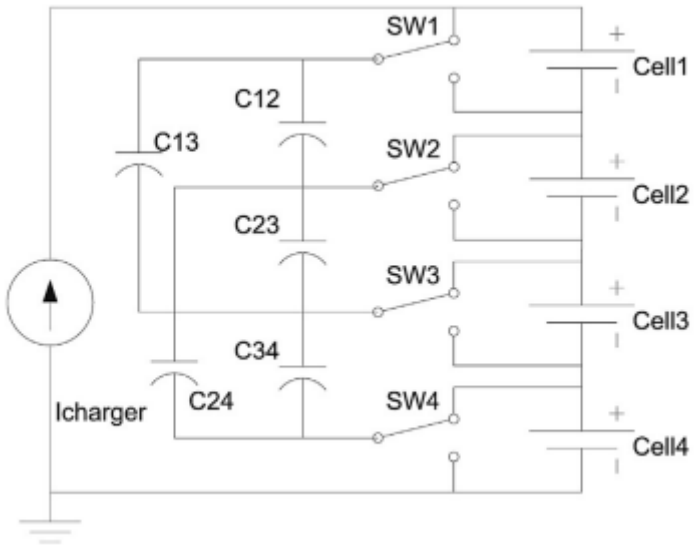

Figure 2.8: Double-tiered switch capacitor method (Gallardo-Lozano et al., 2014).

Distinct advantages arise when compared double-tiered switched capacitor to the single-tiered switched capacitor method, primarily in terms of balancing speed and reduced currents across the balancing capacitors. Moreover, it achieves a simultaneous increase in charge transfer along the cell string. This is a result of enhanced charge distribution between the cells with the highest and lowest charge levels. However, it's important to acknowledge the downsides, including higher costs and increased size associated with this approach (Gallardo-Lozano et al., 2014).

2.4.2 Transformer Based Cell Balancing

Transformer based cell balancing uses transformer as power distribution to individual units, cells, and components within a system. This approach offers various iterations, including the use of multiple transformers, transformers with multiple auxiliary windings, and a single transformer switch across cells. In the case of employing multiple transformers as shown in **Figure 2.9**, their primary windings are interconnected correspondingly, while each secondary winding is connected to a distinct cell via transistors. A switch connects the main winding to the pack voltage, resulting in power transmission to each unit with a 50% duty cycle (Gallardo-Lozano et al., 2014).

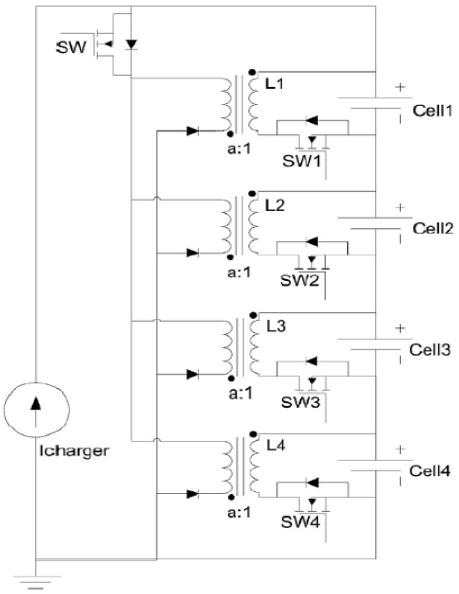

Figure 2.9: Transformer based cell balancing using multiple transformers (Gallardo-Lozano et al., 2014).

Alternatively, the multi-auxiliary winding transformer technique utilizes a single transformer with multiple auxiliary windings, eliminating the need for numerous transformers. The balancing process remains consistent, though the number of secondary windings becomes a limiting factor for the total cell count in this approach. In the single transformer method, a sole transformer with multiple secondary windings is cycled across cells to provide energy to weaker cells until equilibrium is reached. Although this switched transformer method is more compact, it requires a sophiscated control system to ensure proper cell equalization than the other transformer-based circuits (Gallardo-Lozano et al., 2014).

2.4.3 Converter Topology-Based Cell Balancing

Cell balancing can also be accomplished using widely-used dc-dc converter configurations including bidirectional buck-boost, bidirectional Cuk, bidirectional flyback, full-bridge, and quasi-resonant converters. The adoption of converter-based cell balancing has gained popularity in recent times due to its distinctive capability to oversee the entire balancing procedure. However, significant challenges still persist due to system complexity and high cost (Habib et al., 2023). Typically, each cell is equipped with a single converter,

enabling electricity transfer between adjacent cells. Unlike previous methods that primarily focused on voltage alignment, these converters possess the capability to control energy movement according to instructions from the BMS. This flexibility provides enhanced autonomy in managing the SoC of cells. **Table 2.1** presents a comparison of various converter-based cell balancing strategies, highlighting the active components used in each strategy, along with their respective advantages and disadvantages. (Bashir et al., 2022).

Table 2.1: Comparison of different configurations of converter-based cell balancing (Bashir et al., 2022).

Technique	Methodology	Active Element	Advantage	Disadvantage
Common Converter-Based Balancing	Buck-boost converter	N converters	Good efficiency, satisfactory balancing speed	The greater size, cost, and complex control are needed
	Cuk converter	n-1 converters	Good balancing speed, satisfactory efficiency	Complicated control is needed, a large size
	Flyback converter	1 converter, 2n switches, and 1 transformer	fewer components, low complex control, high balancing speed	Transformer needed
	Multi-module full-bridge converter	N converters	scaleable to high power usage, decent balancing speed	big size, costly, and complex control is required
	Quasi-resonant converter	n-1 converter	Easy to implement, high efficiency	Higher cost, size

A double layers active cell equalization with the use of bulk-boost convertor is discussed below. There are two layers in this topology where the inner layer using reconfiguration topology and outer layer using bulk boost convertor. This inner layer helps to isolate the battery with lowest SOC or faulty battery without affecting the overall operation. However, when one cell is isolated, the output voltage becomes smaller hence the output current increases to ensure constant output power. Thus, the outer layer which consists of bulk-boost convertor will realize the balance among battery group and keep the output voltage and power of the system stable (Li et al., 2023). Figure 2.10 shows the schematic diagram of the doble layers active cell balancers.

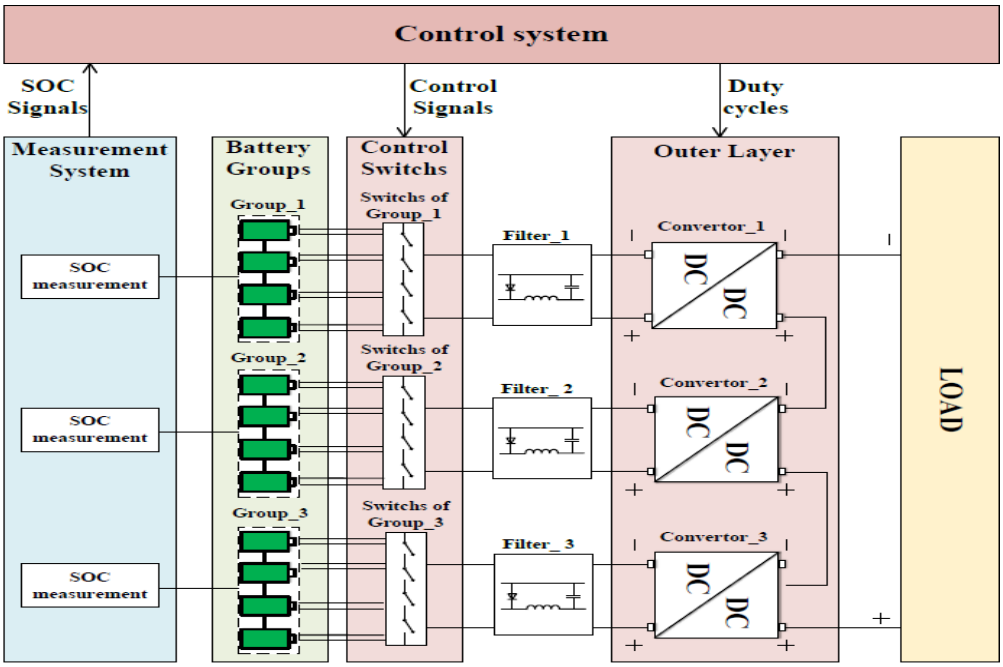

Figure 2.10: Schematic diagram of double layers active cell balancers using bulk-boost convertor (Li et al., 2023).

2.5 Factors Affecting Battery Life Span, Performance And Temperature

There are many factors affect battery life span, performance and temperature. One of the primary factor is due to exposure of overvoltage which lead to the cell degradation. When the batteries in a pack have different SoC, the battery with higher SoC is exposed to higher voltage when charging. This is basically caused by the cell imbalance in the battery pack and when overcharge occurs, it will lead to the increased pressure inside the cell as well as the temperature which lead to explosion or venting (Barsukov, 2023). Besides, the overdischarge of battery will also lead to battery performance and lifespan reduction. Each battery has a specific depth of discharge (DoD), which represents the percentage of its capacity that has been discharged compared to when it is fully charged. It represents how deeply the battery has been discharged during a particular cycle of use. Discharging a battery to extremely low DoD levels can be harmful and lead to irreversible damage (Gailani et al., 2020).

2.6 SoC Estimation

State of Charge (SoC) functions as a relative gauge of the energy stored within a battery. It's quantified as the ratio of the charge that can be withdrawn from the cell at a given time to the total capacity. There are several methods available to estimate battery State of Charge (SoC), including voltage-based SoC estimation (using voltage as a reference and calibrated against SoC), Coulomb counting, and measurement methods based on Kalman filters or Extended Kalman filters. Among these methods, the KF approach stands out for its superior accuracy in SoC determination (Chung & Yang, 2018). Meanwhile, the CC method is the simplest and still offers commendable accuracy compared to the voltage translation method.

2.6.1 Coulomb Counting Method

The Coulomb counting method emerges as the simplest approach for estimating battery SoC. Its implementation is straightforward and demands minimal computational power. This technique relies on the integration of battery current over time during charging or discharging cycles. The mathematical representation for measuring SoC is outlined in Equation (1). However, it's important to note that this method operates as an open-loop algorithm, lead to inaccuracies of calculation due to factors like uncertain disturbances, noise, temperature variations, and current fluctuations. Uncertainties in the initial SoC value can lead to cumulative errors over time. The accuracy of estimation is also significantly impacted by the quality of the current sensors used, which are susceptible to measurement errors that accumulate. Furthermore, this method requires a full discharge of the battery and periodic capacity calibration to attain maximum capacity, contributing to a reduction in battery lifespan (Hannan et al., 2017).

$$SoC(t) = SoC(t-1) + \frac{1}{C}\int_0^t I(t)dt \qquad (1)$$

SoC (t)	-	Initial SoC
$I(t)$	-	Battery current at time instant
dt	-	Step time
C	-	Capacity of battery in Ah

2.6.2 Voltage Translation Based SoC

Battery cell voltage is a widely used indicator due to its reflective correlation with SoC. The relationship between OCV and SoC is plotted in **Figure 2.11** and it can be observed that the relationship of OCV and SoC is non-linear. Typically, cells with higher voltages tend to possess higher SoC levels. The battery cell voltage can be easily measured through various solutions, making it convenient for BMS. Obtaining the highest, lowest, and average voltages is also straightforward, which promotes the adoption of voltage-based equalization strategies (Chen et al., 2022).

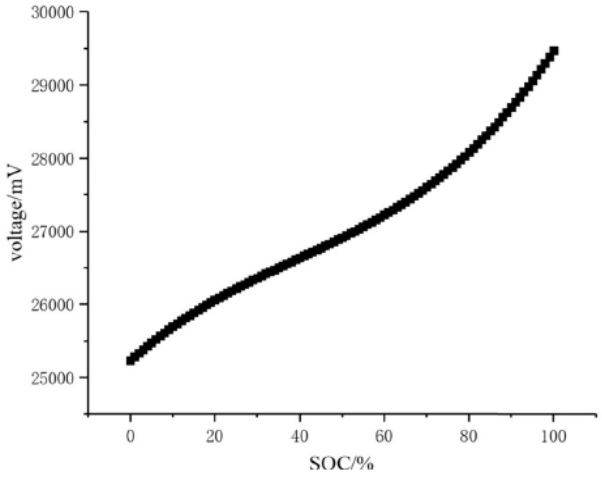

Figure 2.11: Relationship between OCV and SoC (Chen et al., 2022).

For instance, BMS is designed to activate when the voltage difference between the highest and lowest cells exceeds 50 mV, and deactivate when this difference is below 30 mV. However, it's important to note that battery cell voltage is influenced not only by SoC but also significantly impacted by current flow. This means that a battery with a higher voltage might actually possess a lower SoC due to current variations. Since the core principle of battery balancing involves adjusting cell currents, batteries with the same SoC can exhibit different voltages during the balancing process. This discrepancy limits the efficacy of using voltage as the sole indicator for achieving equalization (Chen et al., 2022).

2.6.3 Kalman Filter

The Kalman filter (KF) serves as an intelligent tool for dynamically estimating battery states. It is a well-designed approach that extracts parameters from uncertain and imprecise observations. It is widely used in various domains such as automotive applications, radar tracking, aerospace technology, and navigation tracking. In recent times, the adoption of KF in battery state estimation is successful regardless of its high implementation cost.

A primary feature of the KF is its inherent self-correcting nature, allowing it to manage significant variations in current effectively. Functionally, the KF comprises sets of mathematical equations that continually predict and rectify new states as the system operates. Employing a linear optimal filtering approach, the algorithm provides a recursive solution to estimate state variables. These equations operate within a state-space framework, accounting for the discrete-time representation of cell dynamics.

The core principle of the KF is to compare measured input and output data in order to calculate the minimum mean squared deviation of the true state. This method assumes process noise and measurement noise to be Gaussian, independent, and zero. The KF linear model includes a process equation (Eq 1), which forecasts the current state (xk) based on the preceding state (xk-1), and a measurement equation (Eq. 2), which updates the current state to align it with the actual value.

$$Stateequatiuon : x_{k+1} = A_k x_k + B_k u_k + w_k \quad (1)$$

$$Measurementequation : y_k = C_k x_k + D_k u_k + v_k \quad (2)$$

where 'x' represents the system state, 'u' denotes the control input, 'w' accounts for process noise, 'y' signifies measurement input, and 'v' encompasses measurement noise. The matrices 'A', 'B', 'C', and 'D' are covariance matrices, exhibiting time-varying characteristics that outline the system's dynamics (Hannan et al., 2017).

2.7 Summary

This chapter studied and reviewed past researches on the battery types, cell balancing techniques, factors affecting the battery lifespan, performance and temperature and different methods of SoC estimation. Each section was

discussed and explained in-depth to provide a comprehensive overview of the knowledge behind this project, which also highlighting the current development related in this field. The LIBs has become the most popolar choice among other battery type due to its high energy density, safety and long lifespan. Both passive and active cell balancers are remained widely used in today's industry with the choice of the method depending on system requirement. The main factors which lead to cell degradation are primarily due to overchargiing and overdischarging resulting from cell imbalance. To solve the cell imbalance,it is crucial to determine the SoC of the battery. There are several ways to estimate SoC including CC, voltage translation and KF.

CHAPTER 3

METHODOLOGY AND WORK PLAN

3.1 Introduction

In this chapter, the implementation of the cell monitoring system will be discussed thoroughly, with the main parameter to be considered being the battery's SoC. Various sensors are employed in the system, including voltage sensors, current sensors, and temperature sensors. The voltage will be used as the main indicator to estimate the battery SoC in three cases: during steady state, charging and discharging. A smart charger will be used to achieve constant current constant voltage (CCCV) charging scenario and a load tester will be used to discharge the battery,

The battery type used in this project is a LiFePO4 battery with a nomimal voltage of 3.2V and a specified capacity of 3.4 milliampere-hours (mAh). The battery configuration consists of two modules, each module with a 4S1P arrangement, meaning 4 batteries are connected in series as a module. A battery system is obtained by combining these two modules in parallel. To monitor the battery's voltage comprehensively in different levels, it is crucial to strategically place sensors at the cell level to system level. After obtaining the voltage of each individual battery cell, the microcontroller will provide the feedback to the cell balancing system to balance the cell's voltage.

3.2 Block Diagram of Overall System

The block diagram of cell balancing system with multiples level monitoring system can be observed from **Figure 3.1**. The system consists of a Arduino Mega 2560 as a microcontroller to obtain the reading from different sensors and it will process the voltage of each battery in the battery modules so appropriate response can be given to control the cell balancing circuits. The sensors consist of current, voltage and temperature sensors where they are integrated into the battery modules for measurement. The cell balancing circuit is a switching capacitor active balancer circuit and it will receive the feedback from the microcontroller so it will transfer the energy from high voltage

battery to the low voltage battery. The values from each of the sensors will be displayed via a dashboard using Node-RED and the voltage obtained from the microcontroller will be loaded into a CSV file for further analysis of the result of the proposed balancer circuit.

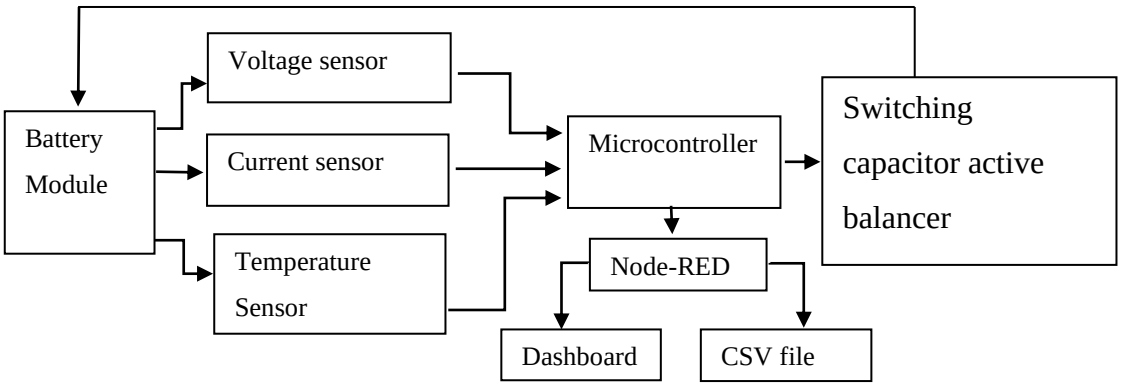

Figure 3.1: Block Diagram of Overall System.

3.3 Battery Configuration

The battery type used in this project is lithium iron phosphate with a nominal voltage of 3.2V and capacity of 3400 mAh. The battery module is configured at 4S1P which consists of four batteries connected in series. Two of these modules will be connected in parallel to form a battery system and to achieve an output voltage of 12.8V and a capacity of 6800 mAh. The battery is soldered using nickel sheet rather the direct silicon soldering to prevent the chance of damage, as shown in **Figure 3.2**.

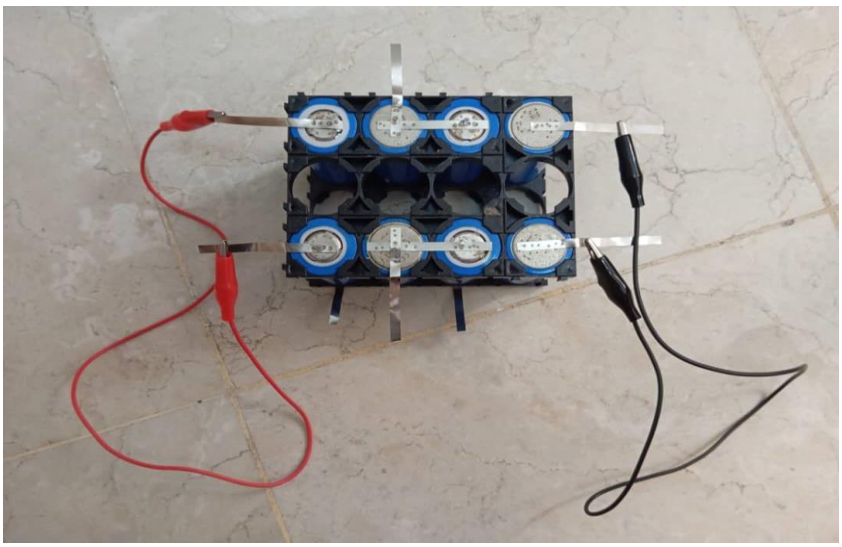

Figure 3.2: Battery configuration.

3.4 Hardware Description

In this section, the details of the hardware to be used in the cell monitoring system and active balancer will be discussed thoroughly. This includes the specification of the hardware as well as their functionalities in the cell monitoring system and active balancer.

3.4.1 Arduino Mega 2560

The Arduino Mega 2560 is a microcontroller board that is based on the ATmega2560 chip as its central component. It has 54 digital input/output pins in which 15 of them can be used as PWM outputs). Besides, it offers 16 analog input channels, features 4 UARTs for hardware serial communication,and incorporates a 16 MHz crystal oscillator and a USB connection. The pin configuration of Arduino Mega 2560 is shown in **Figure 3.3**. The Arduino Mega 2560 is utilized to read sensor values from the cell monitoring system and estimate the SoC of the battery based on the voltage. Once the battery's voltage is known, the microcontroller sends the appropriate response to the cell balancing system to ensure the balancing of all the batteries.

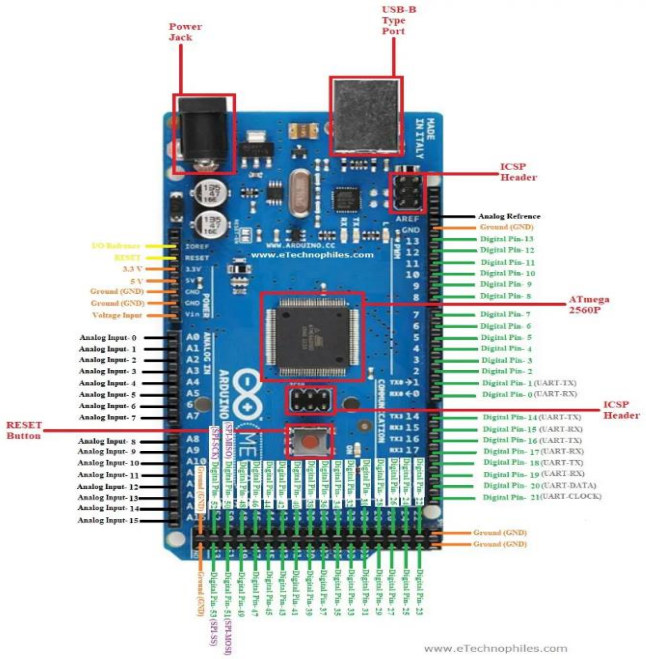

Figure 3.3: Pin configuration of Arduino Mega 2560 (eTechnophiles, n.d.).

3.4.2 NTC Thermistor

The NTC thermistor as shown in **Figure 3.4** stands for Negative Temperature Coefficient thermistor, meaning its resistance decreases as the temperature rises. The thermistor is epoxy coated, which provides its excellent mechanical strength and protection against moisture, physical damage, and chemical. It is small in size which is suite in the BMS and has a fast thermal response time. It can measure a wide range of temperature from -40 degree to 105 degree. The purpose of using NTC thermistor is to determine the temperature of battery when it is charging and discharging so that the battery behaviour can be observed.

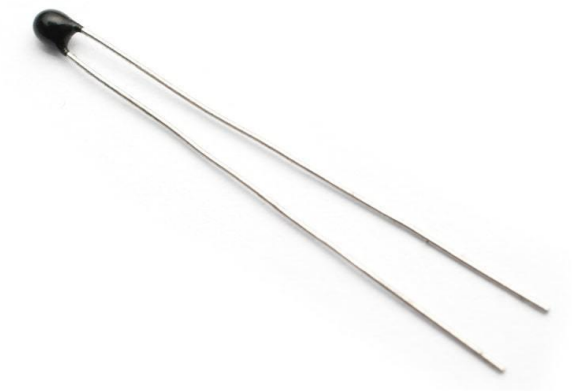

Figure 3.4: NTC thermistor (Storto, n.d.).

3.4.3 Shunt current sensor

The shunt current sensor, as shown in **Figure 3.5**, is a type of sensor used to measure electrical current by detecting the voltage drop across a shunt resistor. The shunt resistor used is normally a low resistance devices in series with the current path. Its operational principle involves the generation of a voltage drop across the shunt resistor that is proportional to the current passing through it, as described by Ohm's Law (V = IR), when current flows through the resistor. By measuring this voltage drop, the shunt current sensor can determine the current flowing through the circuit. This sensor requires a 5V power supply and features an I2C communication with microcontroller. It can measure the voltage up to +26V thus a currents up to 3.2 amperes The purpose of using the

shunt current sensor is to observe the current of each battery module during charging and discharging.

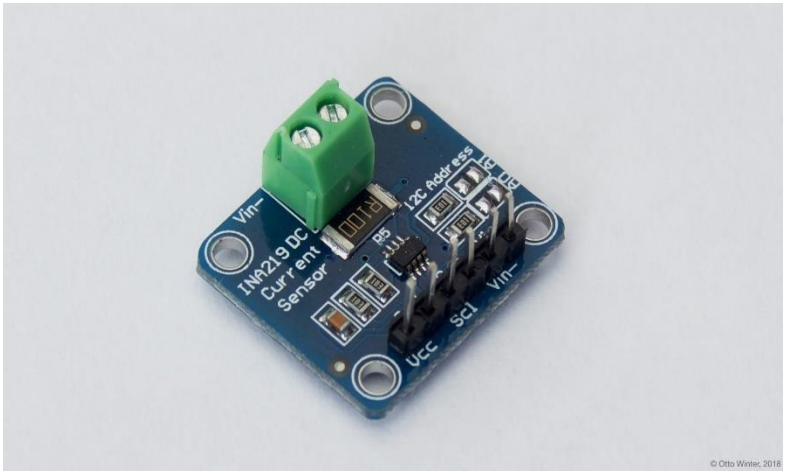

Figure 3.5: Shunt current sensor (ESPHome, n.d.).

3.4.4 Voltage Sensor

The voltage sensor or voltage detector module as shown in **Figure 3.6**, is a device used to measure and monitor voltage levels in electrical circuits. It operates on the principle of a resistive voltage divider and it is designed to reduce higher input voltage to a level that is within the acceptable range of a arduino microcontroller which is 5V. The accuracy of the voltage sensor used is only up to 0.0245V so it might limit the accuracy of the overall result. The voltage sensors are used in cell level, module level and system level to measure the voltage of battery during charging and discharging so that the battery's SoC can be estimated.

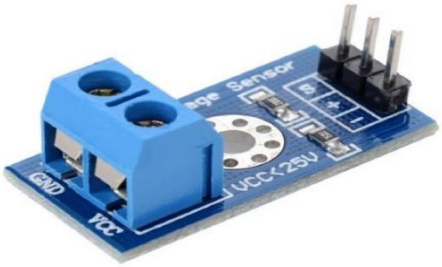

Figure 3.6: Voltage sensor (cablematic, n.d.).

3.4.5 Supercapacitor

Capacitor has a number of advantages compared to battery because it stores energy in the form of an electric field rather than a chemical field. Hence, the long-term loss in storage capacity is substantially lower than that of batteries. Aside from that, capacitors have a higher power density than batteries due to energy storage in the form of an electric field. Supercapacitor as shown in **Figure 3.8** will be used in this project to achieve the energy shuttling between the supercapacitor and battery. The main difference between supercapacitor and regular capacitor is that supercapacitor has high energy storage capacity, voltage rating and lifespan which make them more suitable for the design of a BMS.

Figure 3.7: Green-Cap supercapacitor, 2.7V 500F (Banggood, n.d.).

3.4.6 Electromechanical Relay

Electromechanical relay is used in the switching process for energy transferring between battery and supercapacitor in cell balancing process. The electromechanical relay used in this project is a 8 channels relay module as shown in **Figure 3.8** so that it can be used together with 4 batteries in a balancer. The relay is switched on by applying a 5V voltage to the respective pin number from the digital pin of microcontroller, and the module is powered up using an external DC power supply to ensure it operates efficiently. The reason of using electromechanical relay is that there is no need for the fast switching in the proposed balancer and the slow transfer of charge between supercapacitor and battery.

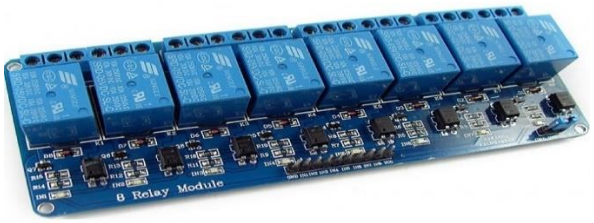

Figure 3.8: 4 channels relay module (Hubtronics, n.d.).

3.5 Software Description

In this section, the details of the software to be used in developing the cell monitoring and balancing system will be discussed thoroughly. There are three softwares to be used, which are the Arduino IDE, Node-RED, and MATLAB Simulink.

3.5.1 Arduino IDE

The Arduino Integrated Development Environment (IDE) is software that includes a built-in script or text editor, allowing users to program and interact with a microcontroller by writing code in the C++ programming language. It is widely chosen in programming microcontrollers because it is free, open source, and its built-in libraries can be easily accessed, which simplifies the coding work. The Arduino IDE is used together with the Arduino Mega 2560 to read the sensors' value and give appropriate respond to control the cell balancing circuit.

3.5.2 Node-RED

Node-RED is an open source programming tool for visual programming that is widely used for connecting Internet of Things (IoT) devices, APIs, and various data sources together. It provides a web-based interface for creating and deploying applications by wiring together nodes to define the logic and data flow of a project. It is available on different operating system such as Windows, macOS, Linux and also Raspberry Pi OS. It is widely used in IoT (Internet of Things) and data integration for real-time data collection, serving as a central

component for managing data transmission across the entire system. For this project, Node-RED will be combined with the Arduino Mega 2560 to facilitate the sending and receiving of sensor data over a USB connection using the serial port. Furthermore, a graphical user interface will be created on Node-RED for reading display and the data obtained will be loaded into CSV file for further result analysis.

3.5.3 MATLAB Simulink

MATLAB Simulink is a companion product to MATLAB and a powerful tool specifically designed for modelling, simulating and evaluating dynamic systems. Simulink is a popular choice for engineers and researchers in a variety of domanins, including control systems, signal processing, and dynamic simulation. It uses a graphical interface to allow users to generate block diagram that reflect a system's behaviour. The use of MATLAB Simulink in this project is to verify and test the functionality of the proposed cell balancing circuit. Besides, it allows the observation of charging and discharging curve of battery during cell balancing, facilitating further investigation.

3.6 Hardware Implementation

Figure 3.9 shows the implementation of battery management system which consists of voltage, current and temperature sensors, battery modules, supercapacitors, electromechanical relays, an external power supply, a load tester and the use of Node-Red for data display. The figure depicts only one battery module of 4S1P, as the results are expected to be the same with the use of two modules connected in parallel. This arrangement simplifies the illustration of the overall system, as the system would be extremely complicated to observe with many components.

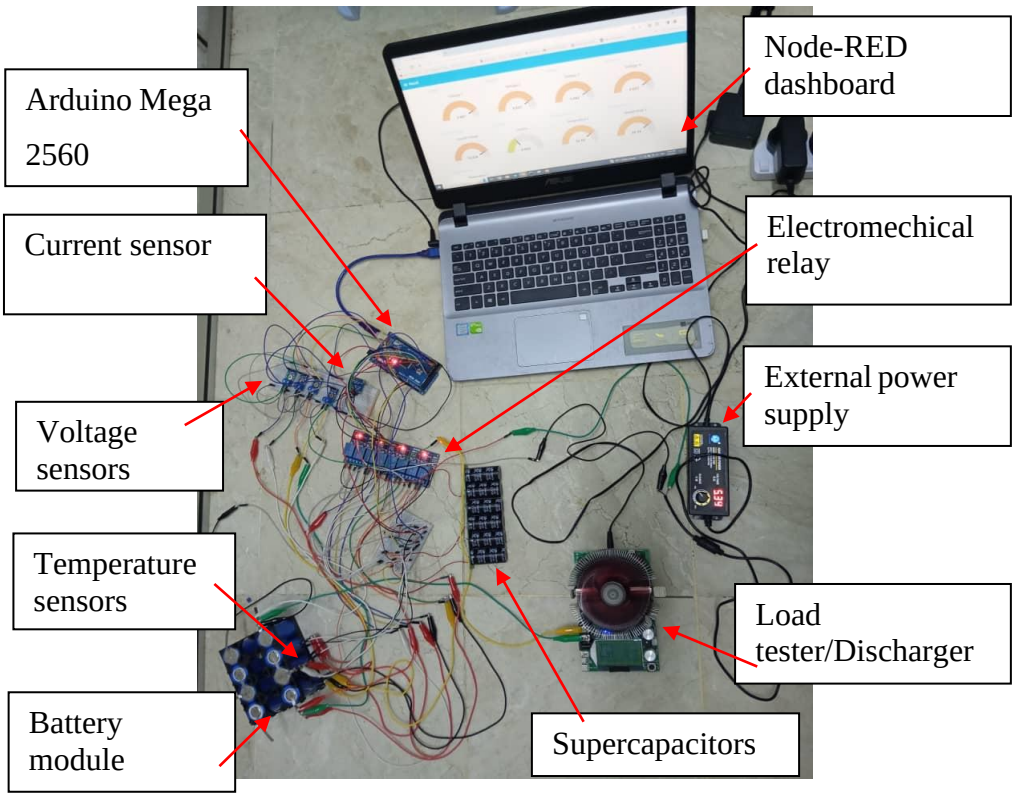

Figure 3.9: Hardware implementation of BMS.

There are total of 8 NTC 10kΩ thermistors used to measure the temperature of each batteries. The thermistors are attached to the batteries via tape, with their tips in close contact with the battery body as shown in **Figure 3.10**. Each of them is connected in series with a 10kΩ resistor and a 5V voltage supply is applied across them. The point where they connected in series is connected to the ADC pin of the Arduino Mega to read the temperature of the battery,

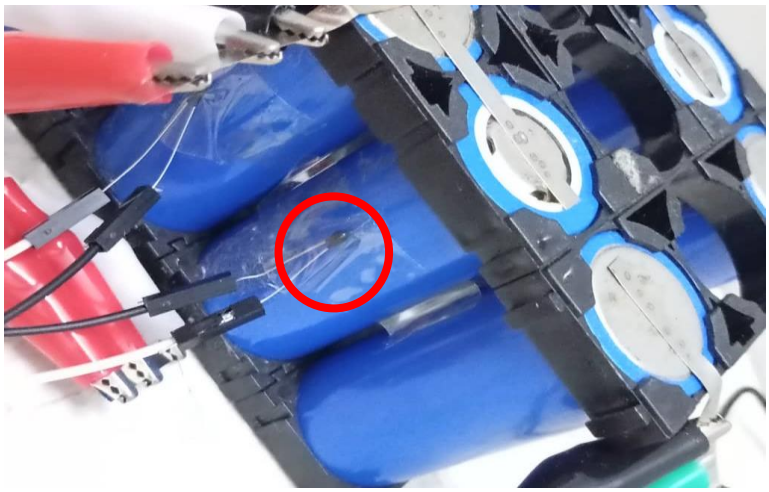

Figure 3.10: Thermistor taped to the battery body.

Similarly, for voltage measurement, 8 voltage sensors will be used to monitor the battery's voltage during charging and discharging. The voltage sensors are connected in a way that they measures the first battery voltage, and the sum of the first and second battery voltages. The second battery voltage is obtained by subtrating the sum of the battery voltage from the first battery voltage. This arrangement is intended to solve the problem of common ground issue across the resistor in the voltage sensor so that the voltage reading can be obtained correctly. The current sensor is connected in series with the load tester or BMS charger to obtain the current of battery module during charging or discharging. **Figure 3.11** shows the use of voltage and current sensor in the the BMS system and **Figure 3.12** and **Figure 3.13** show the detailed connection of the sensors in the hardware implementation.

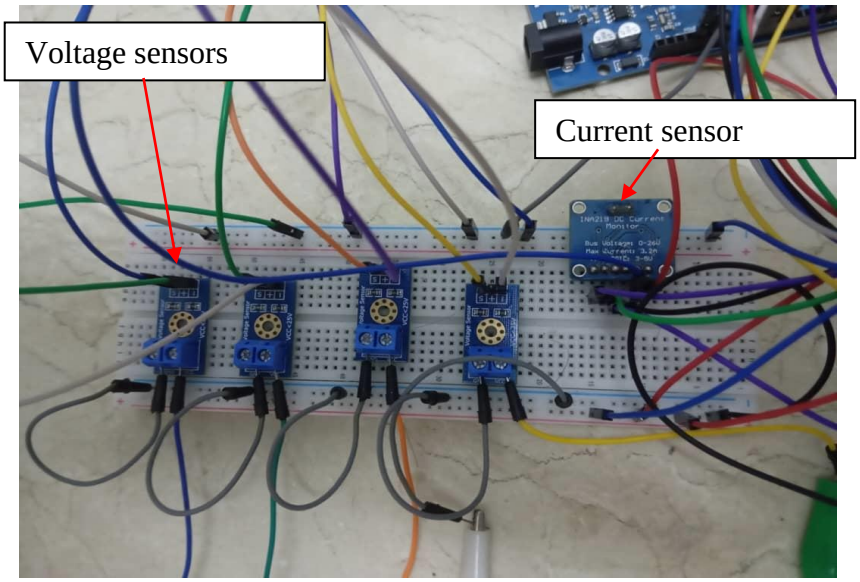

Figure 3.11: The voltage and current sensors used in the BMS.

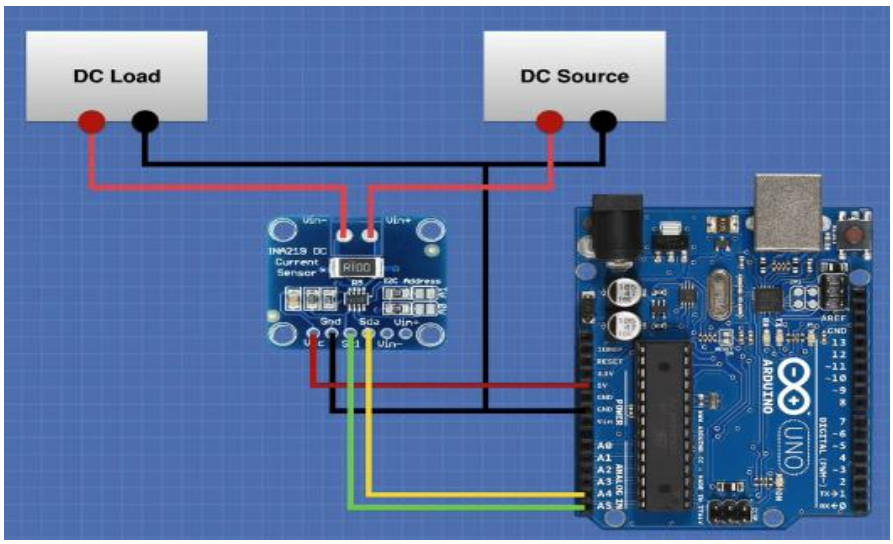

Figure 3.12: Details connection of the current sensor (Dronebot Workshop, 2021).

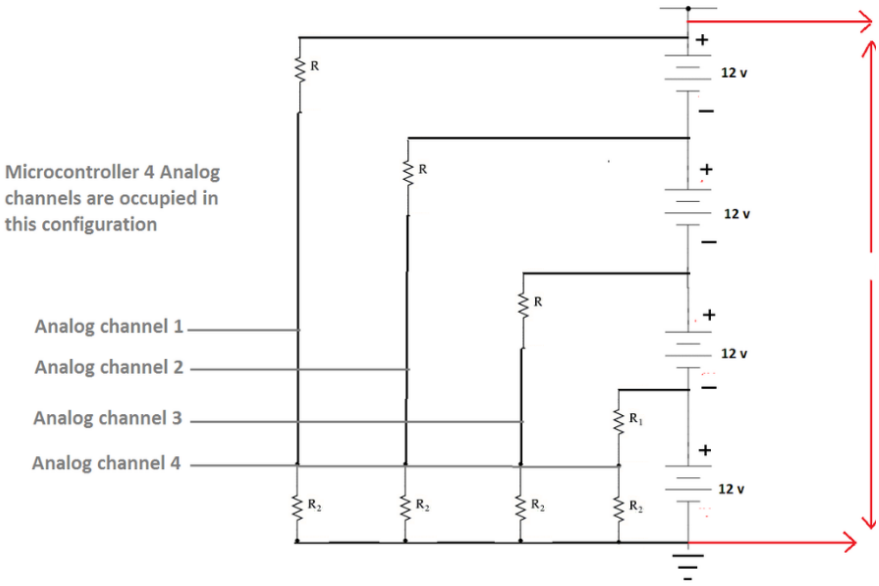

Figure 3.13: Details connection of the voltage sensors (EngineersGarage, n.d.).

The proposed cell balancing circuit is the single-tiered switching capacitor which can be observed from **Figure 3.14**. The 4S1P battery configuration is considered one module and each battery will transfer energy to perform cell level balancing using an external energy storage element which is a supercapacitor in this project. The capacitor switching balancer controlled strategy is simple as the control of switch can be executed using microcontroller and the sequential energy transfer between cells is

accomplished by frequenctly toggling the switch position between the upper and lower position or vice versa.

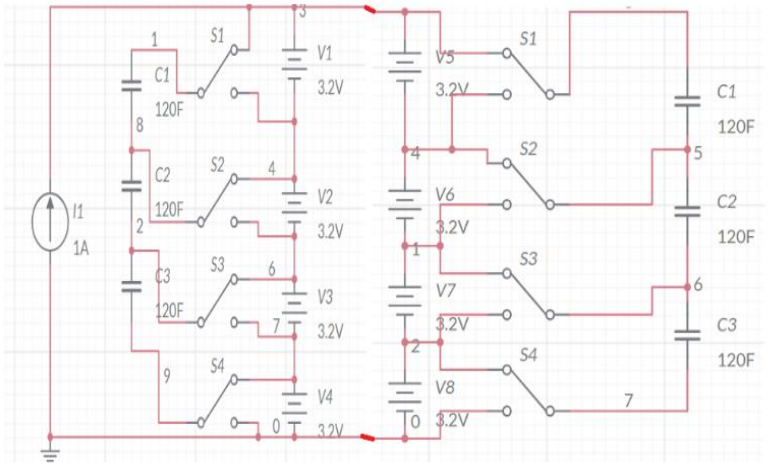

Figure 3.14: Switching capacitor active cell balancer.

The supercapacitor used in this project is a module consisting of six supercapacitors, with each supercapacitor rated at 2.7V and 120F. Since each battery has a nominal voltage of 3.2V, two supercapacitors are used together to achieve a maximum voltage of 5.4V. **Figure 3.15** shows the connection of supercapacitor module where two supercapacitors are connected to one battery with two wires. Whereas, for the electromechnical relay, they are turned on/off by suppling a digital signal from the microcontroller and their Normally Open and COM sides are connected to battery and supercacitor as shown in **Figure 3.16**.

Figure 3.15: Connection of supercapacitor module.

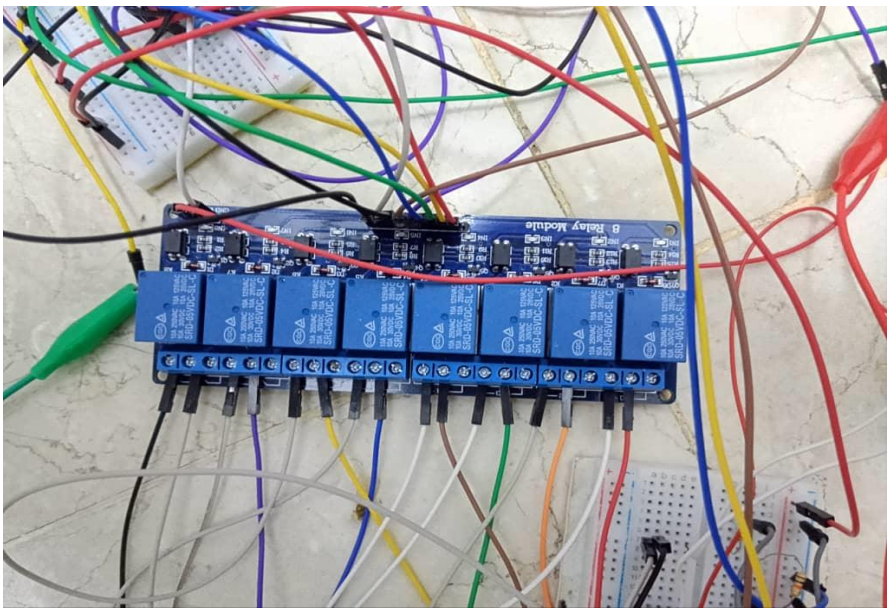

Figure 3.16: Connection of electromechanical relay.

3.7 Software Implementation

The section will discuss about the set up of the Node-RED for data acquisiton from various sensors.

3.7.1 Node-RED Data Acquisition

The configuration of the Node-RED is designed to obtain the values from voltage, current, and temperature sensors. Data transfer from the Arduino Mega to Node-RED is accomplished through the serial port using a USB connection. The configuration is shown in **Figure 3.17**. First, a serial node is selected and dragged into the flow section. The seial node is configured by specifying the serial port to which the Arduino Mega is connected and setting the baud rate to 115200. Next, a function node is chosen where it is programmed to obtain the value from the data received in the serial monitor of the Arduino IDE. The chart node is selected to visualize data values on the Node-RED dashboard. Besides, join and batch nodes are used to collect the voltage and current data into a list, along with the CSV and Write to File nodes, to load the data into a CSV file for further result analysis.

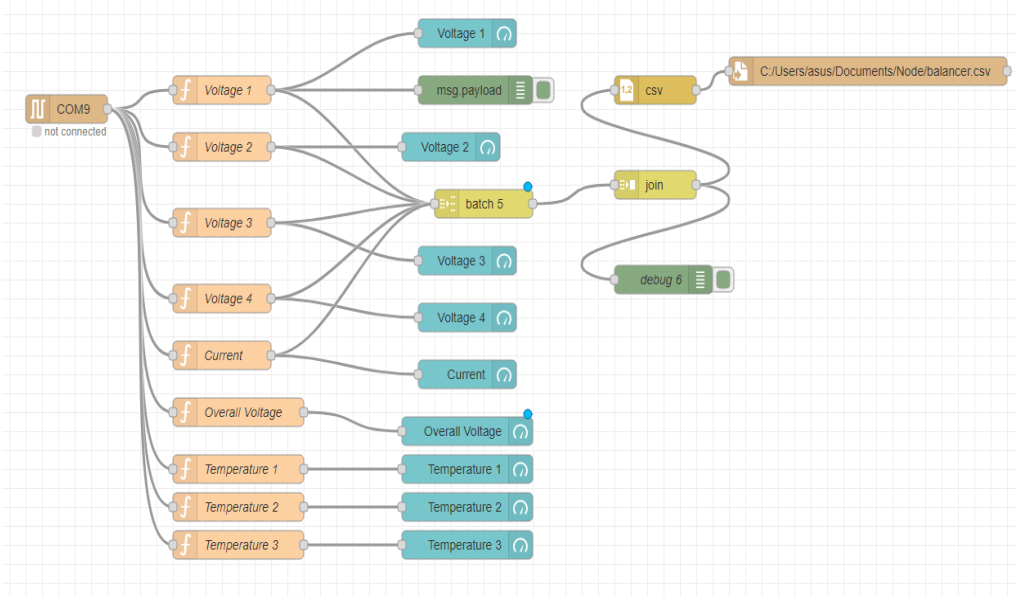

Figure 3.17: Configuration of Node-RED to display data in dashboard and load data into CSV file.

3.7.2 MATLAB Simulink

The switching capacitor active balancer is simulated using MATLAB Simulink to test its functionalities when the battery is in steady-state, charging and discharging. The components used are set with the same parameters used in the practical implementation so that the result can be compared between software simulation and hardware implementation. The relays used in this simulation is ideal switch, and the battery used is lithium battery set to nominal voltage of 3.2V to showcase the use of lithium iron phosphate battery. The supercapacitor is also set to 60uF with no internal resistance given. The State of Charges (SoCs) of each battery are plotted using a scope for three cases: steady-state, charging and discharging, to observe the effects of the active balancer on the batteries themselves. **Figure 3.18** shows the connection of the circuits in MATLAB Simulink.

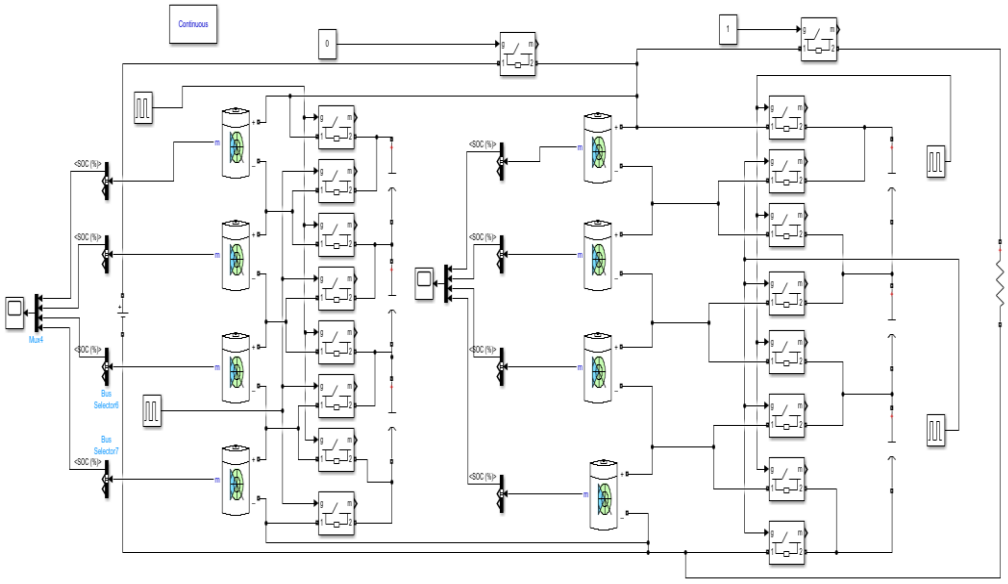

Figure 3.18: MATLAB simulation of switching capacitor active balancer.

3.8 Summary

This chapter covers the necessary hardware and software components for constructing the battery monitoring system and switching capacitor active balancer. It also discusses the implementation approach and the overall system structure. The monitoring system consists of voltage, current and temperature sensors that are read by the Arduino microcontroller and displayed via the dashboard using Node-RED. The switching capacitor active balancer is simulated using MATLAB simulink to test its functionalities in the software simulation. In the hardware implementation, the balancer is constructed using supercapacitors and relays, which are controlled by the microcontroller. The balancer is tested under three cases: steady state, charging and discharging with the battery voltage is logged into a CSV file by using Node-RED for further analysis of results.

CHAPTER 4

RESULTS AND DISCUSSION

4.1 Introduction

This chapter will discuss the implementation of monitoring system for multi-level batteries and the extraction of the data into a CSV file for further data analysis. The results of switching capacitor active balancer will also be compared in both MATLAB simulation and practical implementation. The proposed monitoring system will be discussed for its purpose of obtaining each battery's parameters, as well as its ease and convenience of implementation using Node-RED. The batterries' State of Charges (SoCs) will be used to discuss the MATLAB simulaton, whereas the batteries' voltage will be used to discuss on the practical implementation of the active balancer.

4.2 Charging and Discharging Profile of Lithium Iron Phosphate Battery

It is essential to understand the charging and discharging profile of the battery used in this project before proceeding with the balancer. The battery employed in this project is a lithium iron phosphate (LiFePO4) battery with a nominal voltage of 3.2V and a capacity of 3.4 Ah. The charging profile of the LiFePO4 battery, as illustrated in **Figure 4.1,** involve charging at a constant current of 0.8 A for a duration of 800 seconds, followed by charging at a constant voltage of 3.6V. The battery voltage increases from 2.8 V to 3.2 V, after which it becomes saturated. The current remains at 1.0 A initially and then drops to 0.5A at the end. The discharging profile of the LiFePO4 battery is shown in **Figure 4.2** where the battery is discharged at a load of 1.0 A. It can be observed that the voltage of the battery decreases from 3.2 V to 2.4 V with a constant current of 1.0 A, and the current begins to drop towards the end.

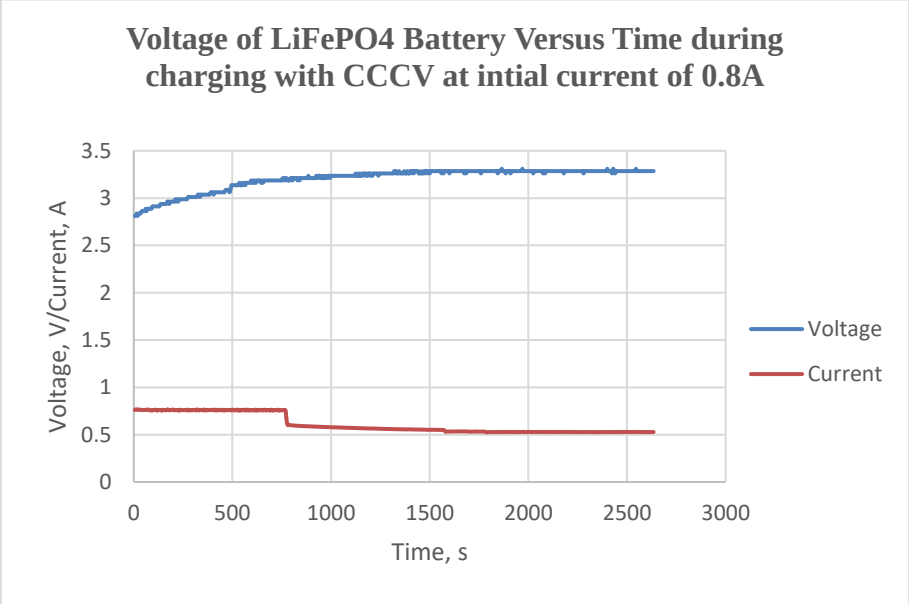

Figure 4.1: Charging of LiFePo4 battery with CCCV at initial current of 0.8A.

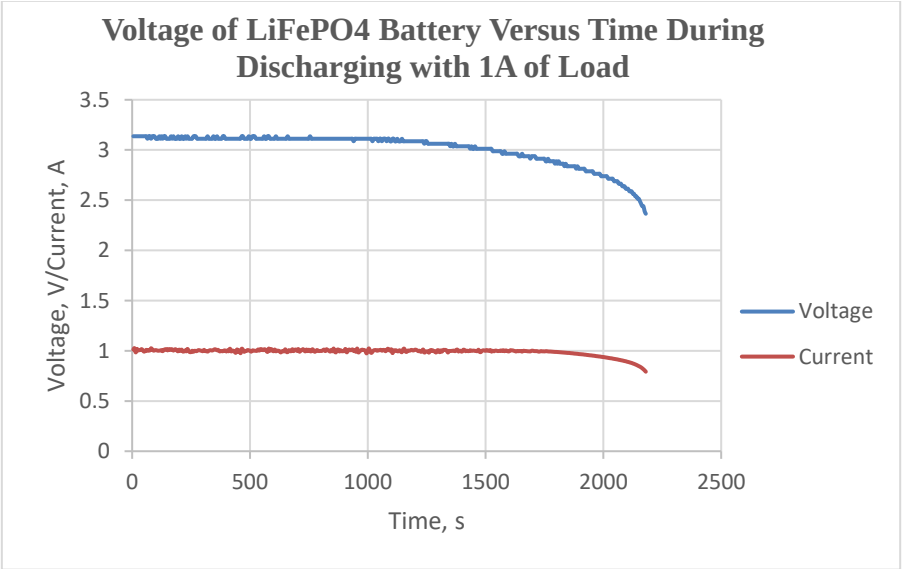

Figure 4.2: Discharging of LiFePo4 battery with 1A of load.

4.3 Monitoring System

Figure 4.3 shows the partial monitoring system implemented by using the dashboard in Node-RED. A battery module which consist of 4S1P was observed to obtain each battery's voltage, overall voltage of battery module, charging current as well as each battery's temperature. The purpose of implementing monitoring system in Node-RED is to replace the serial monitor in the Arduino IDE as shown in **Figure 4.4** for better data illustration. The

range of the data value can be customised in Node-RED according to the requirements, i.e the battery voltage is ranged from 2.6V to 3.6V for the case of lithium iron phosphate battery. The data is extracted by using the function node in the Node-RED to obtain the data printed in the serial monitor of Arduino IDE and load in the the gauge node for display. **Figure 4.5** shows the coding of the function node to obtain the voltage of the first battery.

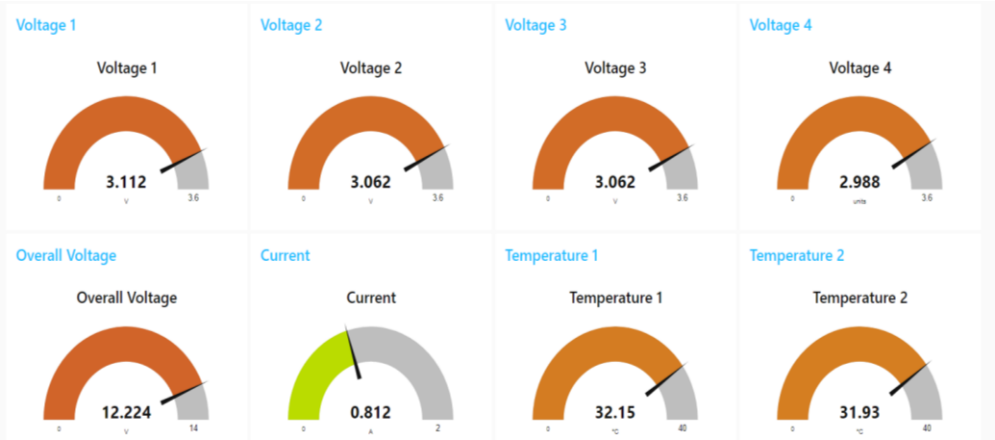

Figure 4.3: Monitoring system displaying various battery parameters.

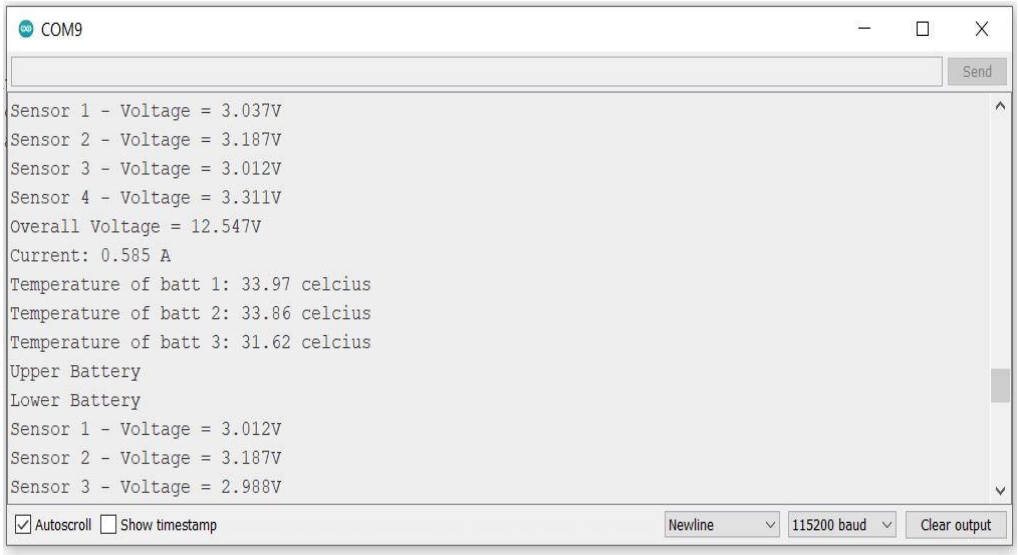

Figure 4.4: Serial Monitor in Arduino IDE.

```
// Assuming msg.payload is a string with the serial monitor output

// Find the index of "Sensor 1 - Voltage =" in the payload
var voltageIndex = msg.payload.indexOf("Sensor 1 - Voltage =");

if (voltageIndex !== -1) {
    // Extract the substring starting from the index of "Sensor 1 - Voltage =" to the end
    var voltageString = msg.payload.substring(voltageIndex + 21, voltageIndex + 28).trim();

    // Parse the voltage value as a floating-point number
    var voltage = parseFloat(voltageString);

    // Create a new payload object with the voltage value rounded to three decimal places
    var result1 = { payload: parseFloat(voltage.toFixed(3)) };

    // Return an array containing the new payload object
    return [result1];
} else {
    // If "Sensor 1 - Voltage =" is not found, return an empty array
    return [];
}

```

Figure 4.5: Coding of function node in Node-RED to obtain data.

4.4 Data Acquisiton

The data obtained from the Node-RED is loaded into CSV file to observe the voltage for each of the batteries during steady state, charging and discharging. For the case of steady state, the data is recorded for every 60 seconds, as it is observed that there is no frequent change in the voltage of the battery. For the case of charging and discharging, the data is obtained for every 30 seconds, as it is observed that there is frequent change in the voltage of the battery. **Figure 4.6** shows the voltage of each batteries with time, along with the discharging current, in different columns of the CSV file.

	A	B	C	D	E	F
1	Time	V1	V2	V3	V4	Current
2	0	3.311	3.286	3.286	3.261	0.673
3	1	3.286	3.311	3.261	3.286	0.661
4	2	3.286	3.286	3.286	3.261	0.664
5	3	3.286	3.286	3.261	3.286	0.666
6	4	3.286	3.286	3.261	3.286	0.669
7	5	3.286	3.286	3.261	3.286	0.663
8	6	3.286	3.286	3.261	3.286	0.665
9	7	3.286	3.286	3.261	3.286	0.666
10	8	3.286	3.286	3.261	3.286	0.665
11	9	3.286	3.286	3.261	3.286	0.664
12	10	3.286	3.286	3.236	3.286	0.664
13	11	3.261	3.311	3.236	3.311	0.661
14	12	3.286	3.286	3.261	3.286	0.666
15	13	3.286	3.286	3.236	3.286	0.663
16	14	3.286	3.286	3.236	3.286	0.665
17	15	3.286	3.286	3.236	3.286	0.666
18	16	3.261	3.311	3.236	3.286	0.664
19	17	3.286	3.286	3.236	3.286	0.664
20	18	3.261	3.286	3.236	3.286	0.665
21	19	3.261	3.286	3.236	3.286	0.665
22	20	3.261	3.286	3.236	3.286	0.662
23	21	3.261	3.286	3.236	3.286	0.667
24	22	3.261	3.286	3.236	3.286	0.664
25	23	3.261	3.286	3.212	3.311	0.663
26	24	3.236	3.311	3.212	3.286	0.665
27	25	3.261	3.286	3.212	3.311	0.664
28	26	3.261	3.261	3.236	3.286	0.666
29	27	3.261	3.261	3.236	3.286	0.665

Figure 4.6: Data Acquisition into CSV file.

4.5 Switching Capacitor Active Balancer Performance Evaluation

4.5.1 Software Simulation

One of the battery modules' State of Charge (SoC) will be showcased to discuss the effect of the switching capacitor active balancer. The batteries in each battery modules are set with different SoC levels which are 80, 70, 60 and 75. The sequence of battery labeling from 1 to 4 is counted from the top battery to the bottom battery, as shown in the MATLAB simulation circuit before. **Figure 4.7** displays the SoC of each battery with the use of switching capacitor balancer during steady state. It can be observed that the SoC of all four batteries converges after 5 hours, with batteries 2 and 4 SoC merging together at the end. When the SoC difference between two batteries is smaller, they tend to balance faster as shown in battery 2 and 4 compare to battery 1 and 3. The result shows that the switching capacitor balancer tends to balance each batteries' SoC but the required time is extremely long.

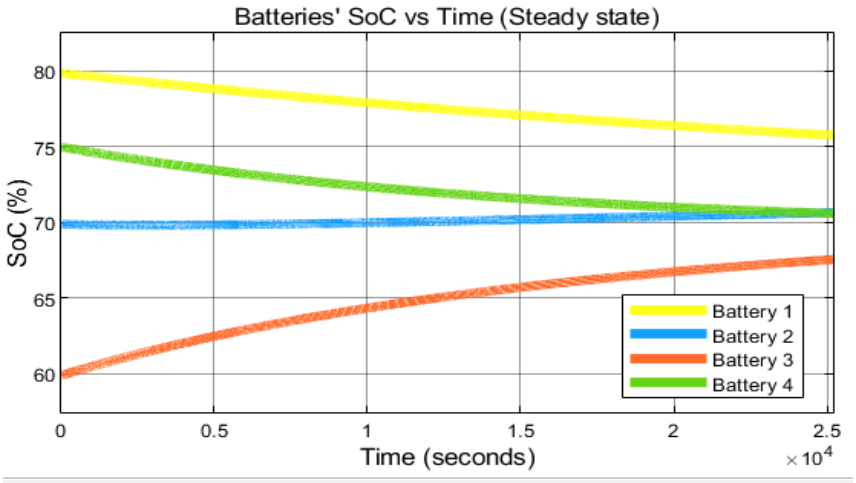

Figure 4.7: Batteries' SoC against time during steady state.

For the case of charging, the same SoC is set for each battery. The battery module is charged at initial current of 1A and 13.9V of DC power supply under CCCV conditon. In order to observe the effect of the balancer on the battery, two graphs are plotted as shown in **Figure 4.8** and **Figure 4.9**. It can be observed that without the balancer, each batteries' SoCs only increases according to its own trend, as shown in **Figure 4.8.** When charging with the

balancer, the batteries' SoCs tend to converge after one hour, which can be observed in batteries 2 and 4 as they start to merge with each other as shown in **Figure 4.9**. Hence, it can be concluded that the balancer also takes effect by attempting to balance the batteries' SoC during charging.

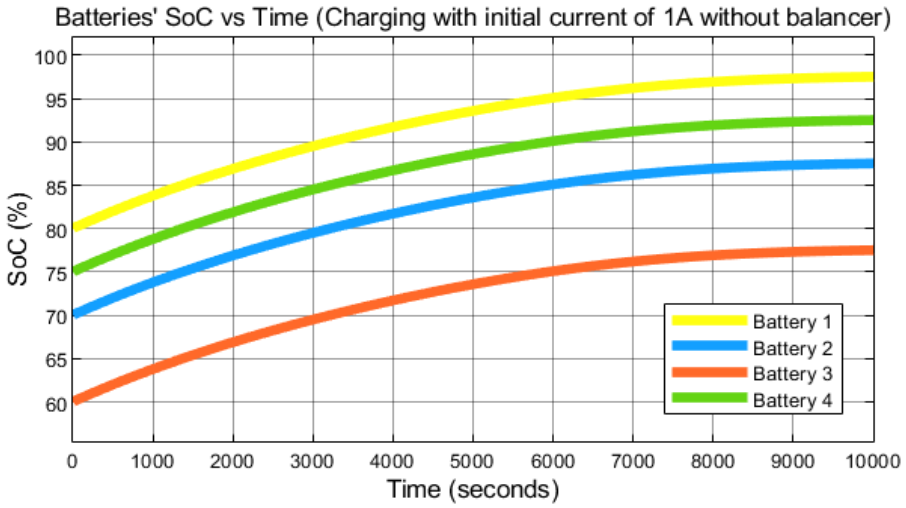

Figure 4.8: Batteries' SoC against time during charging with initial current of 1A without balancer.

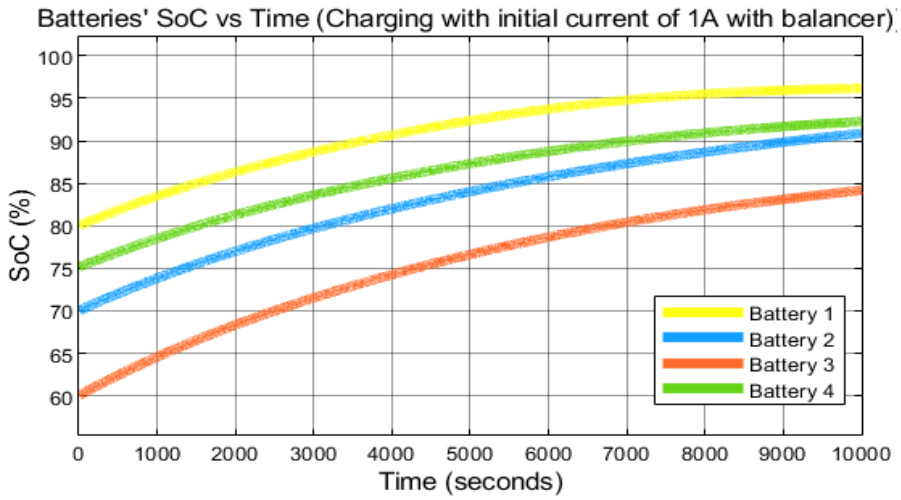

Figure 4.9: Batteries' SoC against time during charging with initial current of 1A with balancer.

For the case of discharging, the same SoC is set for each battery. The battery module is discharged with a load at the current of 0.5A. In order to observe the effect of the balancer on the battery, two graphs are also plotted as

shown in **Figure 4.10** and **Figure 4.11**. It can be observed that without the balancer, each batteries' SoCs only decreases according to its own trend, as shown in **Figure 4.10.** When discharging with the balancer, the batteries' SoCs tend to converge after one and a half hours, which can be observed in batteries 2 and 4 as they start to merge with each other as shown in **Figure 4.11**. In addition, it can be observed that all four batteries' SoC merge together after 4 hours at an SoC value of 20%. Hence, it can be concluded that the balancer also takes effect by attempting to balance the batteries' SoC during discharging.

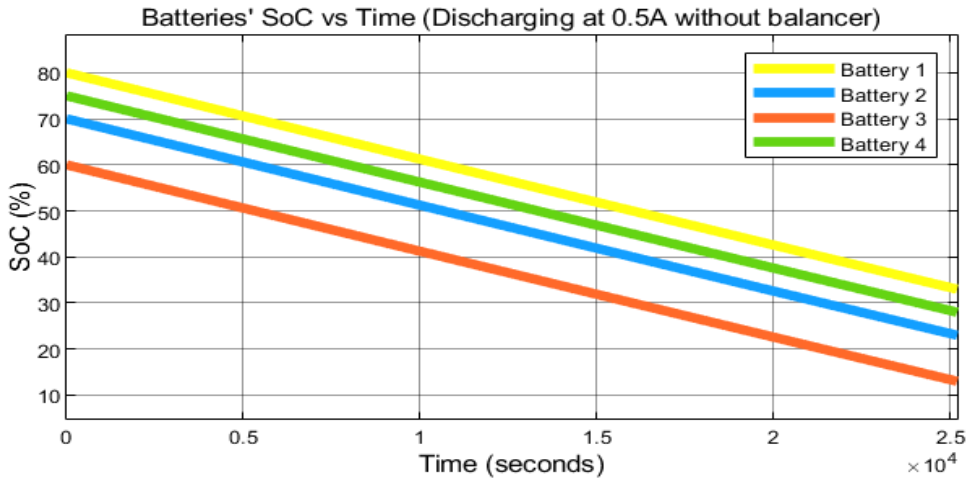

Figure 4.10: Batteries' SoC against time during discharging at 0.5A load without balancer.

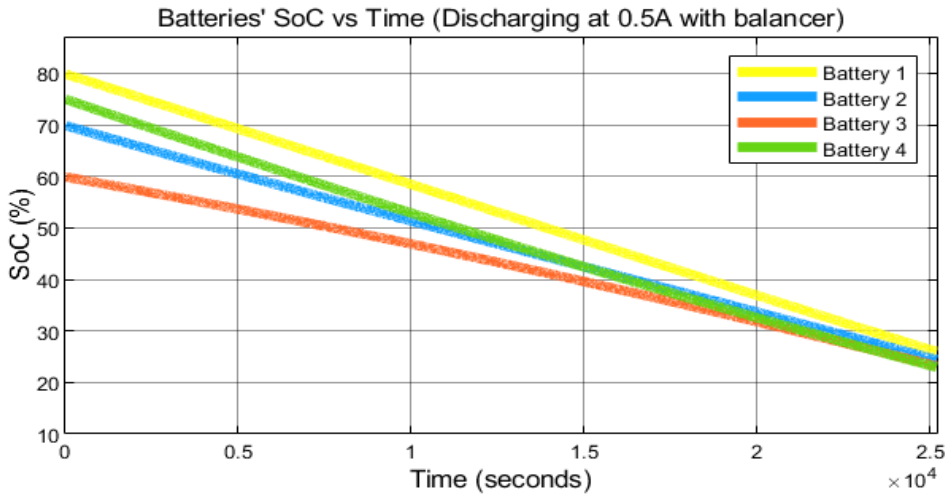

Figure 4.11: Batteries' SoC against time during discharging at 0.5A load with balancer.

4.5.2 Practical Implementation

One of the battery modules' voltages will be showcased to discuss the effect of the switching capacitor active balancer. The reason for using voltage as an indicator is due to its simplicity, and to avoid the use of fuel gauge which uses a combination of voltage, current and temperature measurements along with advanced algorithms to estimate State of Charge (SoC), but it is expensive in nature. The batteries in each battery modules are set with different voltage values to indicate different SoC, ranging from 2.7V to 3.3V. **Figure 4.12** displays the voltage of each battery with the use of switching capacitor balancer during steady state. It can be observed that the voltage of all four batteries converges after 5 hours, with the voltages of batteries 2 and 3 merging together at the end. The middle batteries, which are batteries 2 and 3 can balance faster as they are always connected to the supercapacitor, while the batteries 1 and 4 experience intermittent disconnection from the supercapacitor, leading to a slower balancing process for them. The result shows that the switching capacitor balancer tends to balance each batteries' voltage, but the required time is extremely long.

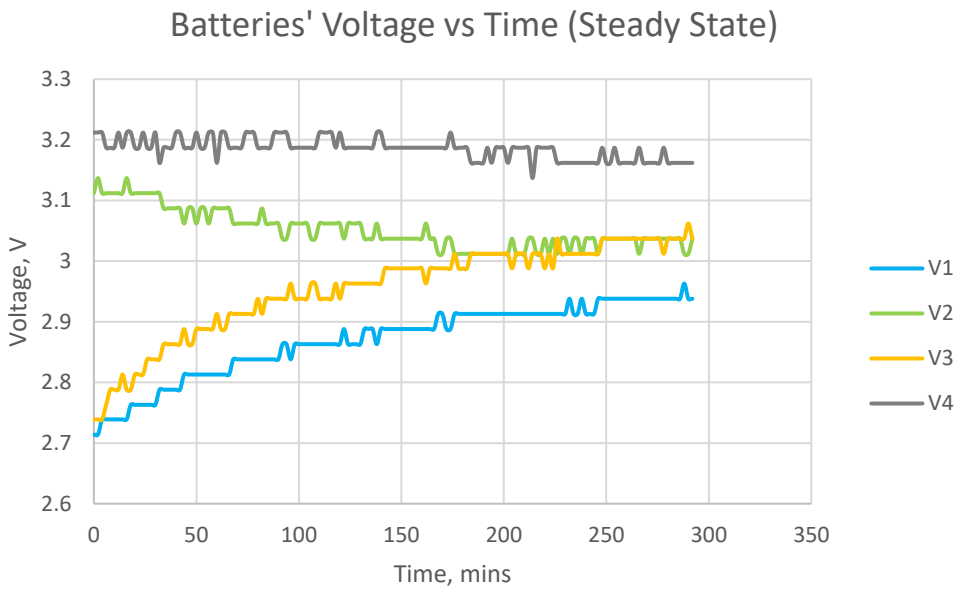

Figure 4.12: Batteries' voltage against time during steady state.

For the case of charging, the voltage is set to the range of 2.9 V and 3.1 V for each battery. The battery module is charged at initial current of 1A and 12.8V with a smart battery charger under CCCV conditons. In order to observe the effect of the balancer on the battery, two graphs are plotted, as shown in **Figure 4.13** and **Figure 4.14**. It can be observed that the batteries' voltages does not converge until they are fully charged with the use of balancer. Each batteries' voltage in both the circuit with or without the balancer increases according to their own trends, as shown in the two graphs. Hence, it can be concluded that the balancer does not take effect in balancing the batteries' voltage during charging.

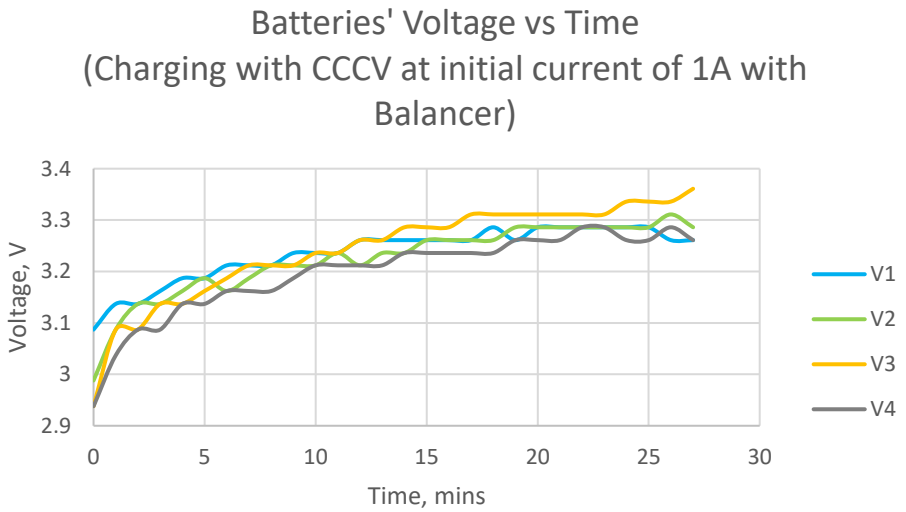

Figure 4.13: Batteries' voltage against time during charging with CCCV at initial current of 1A with balancer.

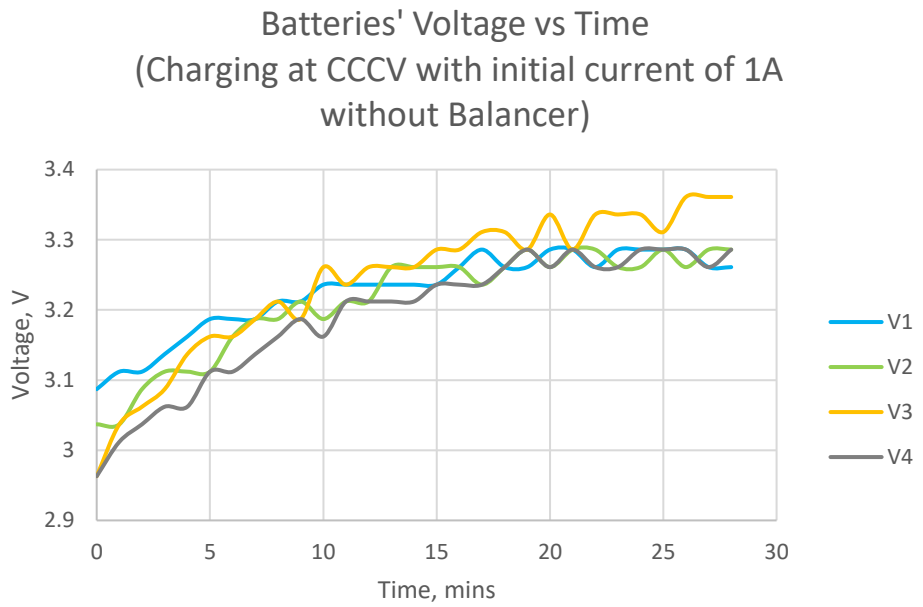

Figure 4.14: Batteries' voltage against time during charging with CCCV at initial current of 1A without balancer.

For the case of discharging, the voltage is set to the range of 3.2 V and 3.4 V for each battery. The battery module is discharged with a load at the current of 0.7A. In order to observe the effect of the balancer on the battery, two graphs are also plotted as shown in **Figure 4.15** and **Figure 4.16**. It can be observed that the batteries' voltages does not converge until they are fully discharged with the use of balancer as the battery 3 is discharged to 2.764 V while the rest of the batteries still discharge at a voltage of 3.262V, as shown in **Figure 4.15**. Each battery' voltage in both the circuit with or without the balancer decreases according to their own trends, as shown in the two graphs. Hence, it can be concluded that the balancer also does not take effect in balancing the batteries' voltage during discharging.

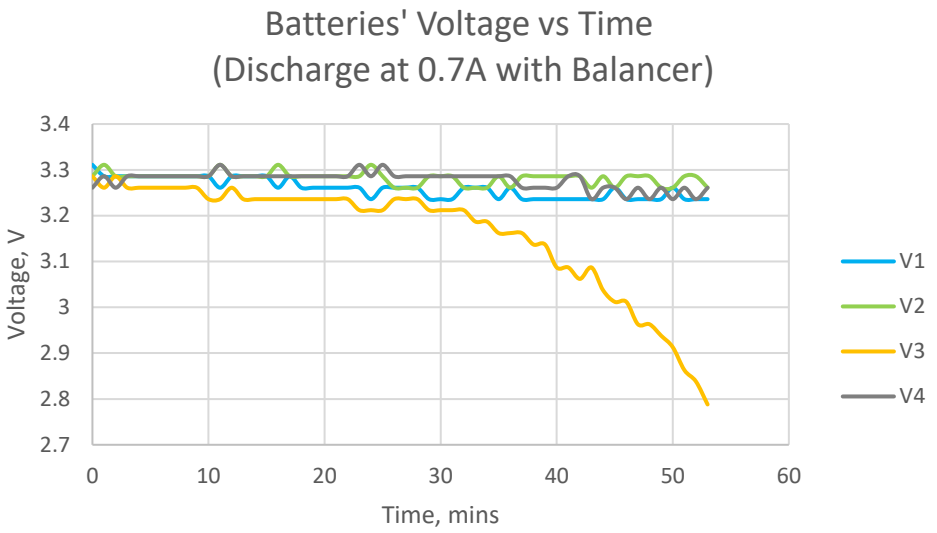

Figure 4.15: Batteries' voltage against time during discharging at 0.7A load with balancer.

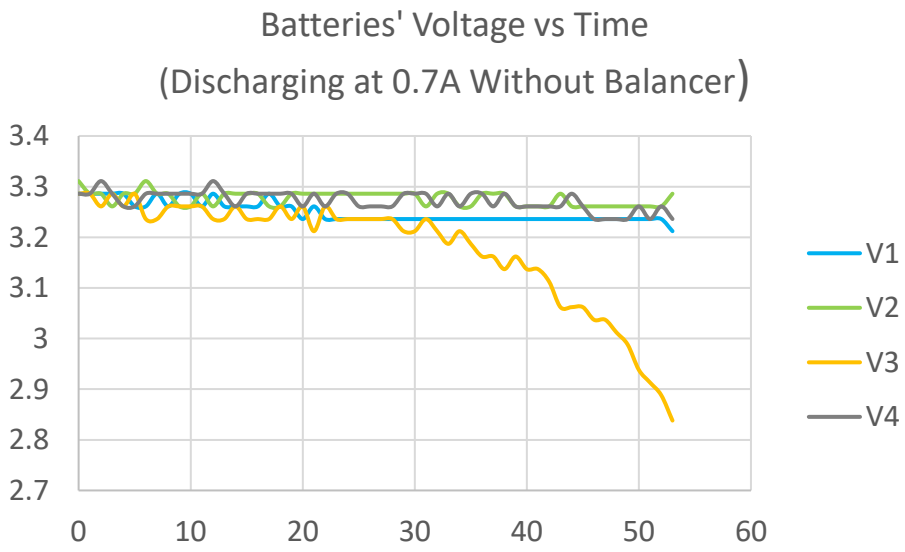

Figure 4.16: Batteries' voltage against time during discharging at 0.7A load without balancer.

4.6 Comparison Between Hardware Implementation and Software Simulation

From the results of both the hardware implementation and software simulation, it can be observed that State of Charge (SoC) is the best indicator to test the functionalities of the switching capacitor active balancer. This is because the batteries tend to balance themselves, as shown in SoC versus time plots in

three different cases: steady state, charging and discharging. However, in the hardware implementation, the batteries only tend to balance themselves during steady state, as shown in voltage versus time plots, whereas they do not balance themselves during charging and discharging. The use of voltage is not a good indicator to observe the State of Charge of the battery as the LiFePO4 battery has an extremely flat voltage across a wide variation of SoC due to its non-linear relation. Hence, it might be that there is a trend of balancing in the batteries, but the use of voltage cannot efficiently prove it.

Furthermore, the software simulation involves the use of ideal switches which lead to no voltage loss. Hence, this will, in turn, increase the effiencicy of the working of the balancer as batteries tend to balance faster. Compared to the hard implementation, the use of electromechanical relays introduces voltage loss which leads to an extremely slow transfer of charge when the voltage of both the supercapacitor and battery are very near. The battery model and supercapacitors used in this project are assumed ideal with minimum or no internal resistance. Hence, this factor will affect the balancing speed, which can be observed in the hardware implementation due to the presence of internal resistance in the LiFePO4 battery and supercapacitor.

4.7 Summary

In summary, the implementation of the monitoring system for multi-level batteries and the switching capacitor active balancer was discussed, along with the extraction of data into a CSV file for further analysis. The monitoring system, utilizing Node-RED, proved effective in obtaining each battery's parameters conveniently. The battery's State of Charge (SoC) was found to be a reliable indicator for testing the balancer's functionalities, especially in MATLAB simulation. However, the hardware implementation showed limitations in balancing during charging and discharging, likely due to the flat voltage profile of the LiFePO4 battery. The software simulation, employing ideal switches, demonstrated faster balancing compared to the hardware implementation with electromechanical relays, which introduced voltage loss. Overall, while the balancer showed effectiveness in balancing SoC in simulation, its practical implementation faced challenges due to internal

resistance in the battery and supercapacitor. Further optimization may be required to improve the balancing speed and efficiency in practical applications.

CHAPTER 5

CONCLUSIONS AND RECOMMENDATIONS

5.1 Conclusions

In conclusion, the proposed monitoring system can display the voltage, current and temperature of the batteries at different levels using the Node-RED dashboard to obtain various batteries parameters such as State of Charge (SoC) and battery health. The use of Node-RED also allows for data acquisition for the result analysis of the proposed switching capacitor balancer. It can be observed that in the hardware implementation of switching capacitor balancer, the batteries' voltages do not converge during charging and discharging because the components used for switching mechanism are electromechanical relays which lead to voltage losses and limit the switching speed. Another factors can be due to the use of voltage as an indicator for SoC and the existence of internal resistance of the battery and the supercapacitor themselves, which lead to slower transfer of charge.

In the software simulation, the batteries' SoC converge during charging and discharging because it is assumed that there is no voltage loss across the relay used, as well as minimum and no internal resistance of the battery and supercapacitor. However, both the software and hardware balancers work with the batteries when they are in steady state. Nonetheless, the balancing speed of the proposed active balancer is extremely slow, and it takes a long duration to balance themselves. The balancing speed can be increased by considering the use of electronic switches to increase its switching speed and minimize losses, but the design of a bidirectional switches need to have a sophisticated driver design, which will be challenging.

5.2 Recommendations for Future Work

It can be observed from the outcome of this project that the use of electromechanical switches affects the balancer's performance in balancing the batteries. Hence, it is recommended to use electronic switches such as MOSFETs and IGBTs to replace electromechanical switches. Electronic

switches can effectively minimise the power and voltage loss and increase the switching speed by setting pulse-width modulation to achive fast balancing. However, in order to allow battery charge transfer to the supercapacitor or vice versa, the switch design must allow for bidirectional flow of current. This can be achieved by connecting both MOSFET switches back-to-back due to the presence of their body diode, which allows for bidirectional flow of current, as shown in **Figure 5.1**. However, designing bidirectional switches requires a sophisticated driver design to ensure that Vgs threshold of the MOSFETs can be reached to ensure they are fully on or off , which can be challenging. Hence, it is recommended to simulate the circuit using any available software tool such as MATLAB simulink to test the functionalities of the circuit before proceeding with hardware implementation to avoid additional cost.

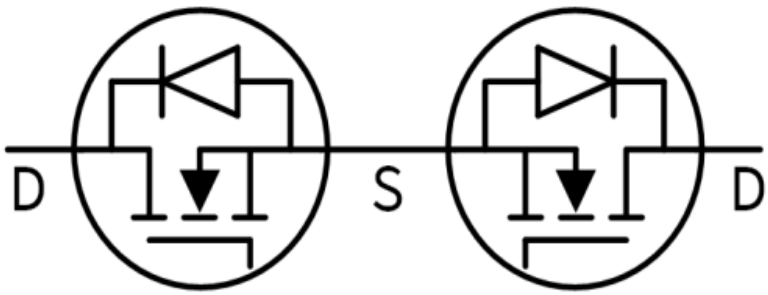

Figure 5.1: Bidirectional power N-MOSFET switches with common source (Infineon, n.d.).

Furthermore, the proposed active balancer is a single-tier switching capacitor which might affect the balancing speed of the batteries. Hence, it is recommended to look for more advanced active balancers with more sophisticated balancing algorithms, such as double-tier switching capacitor balancers, flyback converter balancers, bidirectional multiple transformers balancer and so on. There are also quite a number of improved balancer circuits published on the internet for reference, which is good for exploration. However, when it comes to implementing the proposed circuit in practice, it will be extremely challeging as it requires thorough knowledge when connecting all the components together.

In addition, it is recommended to use of cable ties and connectors, as shown in **Figure 5.2** to minimize the complexity of wiring as observed in the hardware implementation due to the excessive use of wires. This can also prevent the risk of short circuits, which can lead to damage of the components, as they can help organize the wires neatly. The reasons for too much wiring in the proposed syste is due to sensor and balancer connections, and the use of connectors can make them more organized. Besides, each wires can also be identified by labelling them to make it easier for troubleshooting any issues in the future. This also allows for the improvement of the testing scenario as more battery modules can be used.

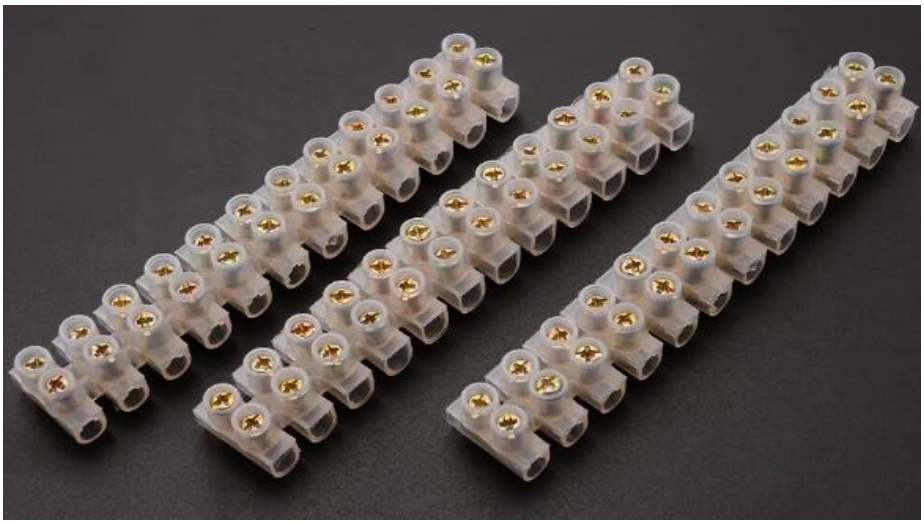

Figure 5.2: Electrical wire connectors strips (AliExpress, n.d.).

On the other hand, the batteries used in this project are old, and their performance might affect the results of the balancer. The old batteries might be short-circuited, overcharged or discharged before, which leads to the variations in their characteristics. Hence, it is recommended to use newly manufactured batteries for testing the balancer. Furthermore, the use of voltage as indicator in the hardware implementation is not a good choice to estimate the battery's State of Charge (SoC) as lithium iron phosphate batteries have an extremely flat voltage across a wide variation of the SoC due to non-linear relation, as shown in **Figure 5.3**. Hence the use of voltage might not accurately observe the effects of the balancer. The use of fuel gauge, as shown in **Figure 5.4** is recommended as it can measure the voltage, current and temperature, and with the use of the advanced algorithms, it can estimate the

battery SoC accurately. However, the trade-off is that the use of a fuel gauge is expensive, so the expense of the overall project must be considered.

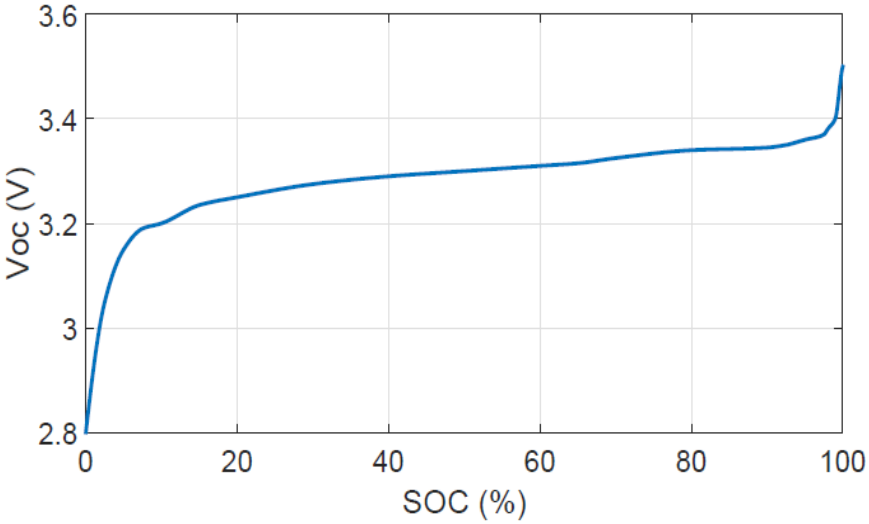

Figure 5.3: LiFePO4 battery voltage versus State of Charge (Hasan, Skriver and Johansen, 2018).

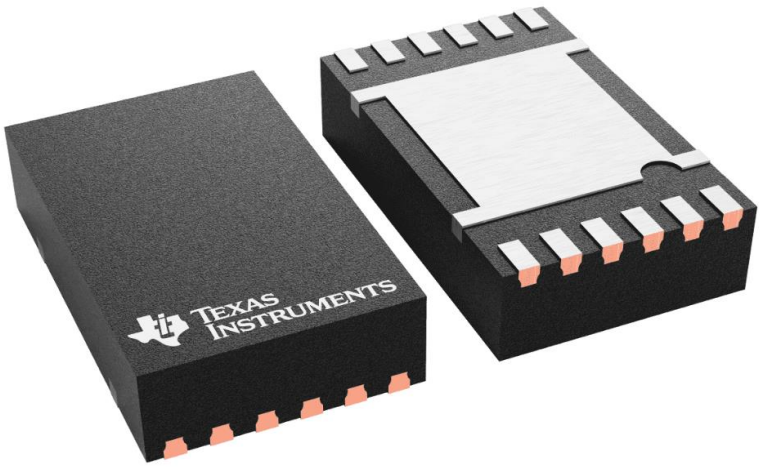

Figure 5.4: BQ27441-G1 single-cell battery fuel gauge (Texas Instruments, n.d.).

REFERENCES

Bashir, H., Yaqoob, A., Kousar, F., Khalid, W., Akhtar, S., & Sultan, W. (2022). A Comprehensive Review of Li-ion Battery Cell Balancing Techniques & Implementation of Adaptive Passive Cell Balancing. *2022 International Conference on Electrical Engineering and Sustainable Technologies, ICEEST 2022 - Proceedings*. https://doi.org/10.1109/ICEEST56292.2022.10077854

Barsulov, Y. (2023). Battery Cell Balancing: What to Balance and How, [online] Available at: <https://www.researchgate.net/publication/265028955_Battery_Cell_Balancing_What_to_Balance_and_How> [Accessed 22 July 2009].

Chen, Z., Liao, W., Li, P., Tan, J. & Chen, Y. (2022). Simple and high-performance cell balancing control strategy. *Energy Science & Engineering*, 10(9), pp.3592–3601. https://doi.org/10.1002/ese3.1243.

Chung, D. W., & Yang, S. H. (2018). SOC estimation of lithium-ion battery based on kalman filter algorithm for energy storage system in microgrids. *E3S Web of Conferences*, *57*. https://doi.org/10.1051/e3sconf/20185702006

Gailani, A., Mokidm, R., El-Dalahmeh, M., El-Dalahmeh, M., & Al-Greer, M. (2020). Analysis of Lithium-ion Battery Cells Degradation Based on Different Manufacturers. In 2020 55th International Universities Power Engineering Conference (UPEC), Turin, Italy (pp. 1-6). https://doi.org/10.1109/UPEC49904.2020.9209759

Gallardo-Lozano, J., Romero-Cadaval, E., Milanes-Montero, M. I., & Guerrero-Martinez, M. A. (2014). Battery equalization active methods. In *Journal of Power Sources* (Vol. 246, pp. 934–949). https://doi.org/10.1016/j.jpowsour.2013.08.026

Habib, A. K. M. A., Hasan, M. K., Issa, G. F., Singh, D., Islam, S., & Ghazal, T. M. (2023). Lithium-Ion Battery Management System for Electric Vehicles: Constraints, Challenges, and Recommendations. In *Batteries* (Vol. 9, Issue 3). MDPI. https://doi.org/10.3390/batteries9030152

Hannan, M. A., Lipu, M. S. H., Hussain, A., & Mohamed, A. (2017). A review of lithium-ion battery state of charge estimation and management system in electric vehicle applications: Challenges and recommendations. In *Renewable and Sustainable Energy Reviews* (Vol. 78, pp. 834–854). Elsevier Ltd. https://doi.org/10.1016/j.rser.2017.05.001

Li, Y., Yin, P., & Chen, J. (2023). Active Equalization of Lithium-Ion Battery Based on Reconfigurable Topology. *Applied Sciences (Switzerland)*, *13*(2). https://doi.org/10.3390/app13021154

Liu, W., Placke, T., & Chau, K. T. (2022). Overview of batteries and battery management for electric vehicles. In *Energy Reports* (Vol. 8, pp. 4058–4084). Elsevier Ltd. https://doi.org/10.1016/j.egyr.2022.03.016

Paidi, R., & Gudey, S. K. (2022). Active and Passive Cell Balancing Techniques for Li-Ion Batteries used in EVs. *2022 IEEE International Power and Renewable Energy Conference, IPRECON 2022*. https://doi.org/10.1109/IPRECON55716.2022.10059573

Pelin, D., Brandis, A., Kovačević, M., & Halak, F. (2022). Design and Testing of a Multimode Capable Passive Battery Management System. *Energies, 15*(12). https://doi.org/10.3390/en15124335

APPENDICES

Appendix A: Arduino Code for Monitoring System and Balancer

```
#include <Wire.h>
#include <Adafruit_INA219.h>

Adafruit_INA219 ina219;

const int voltageSensorPins [] = {A0, A1, A2, A3} ;          // sensor pin
const int numSensors = 4;                                   // Number of voltage sensor
float vIn[numSensors];                                      // Array to store measured voltage
float vOut;
float voltageSensorVal;                   // value on pin A3 (0 - 1023)
const float factor = 5.09375;               // reduction factor of the Voltage Sensor shield
const float vCC = 5.00;                   // Arduino input voltage
const int ThermistorPins[] = {A8, A9, A10, A11};
int Vo;
float R1 = 10000;
float logR2, R2, T;
float c1 = 1.009249522e-03, c2 = 2.378405444e-04, c3 = 2.019202697e-07;
int S1 = 22;
int S2 = 24;
int S3 = 26;
int S4 = 28;
int S5 = 30;
int S6 = 32;
int S7 = 34;
int S8 = 36;


void setup(void)
{
  pinMode(S1, OUTPUT);
  pinMode(S2, OUTPUT);
  pinMode(S3, OUTPUT);
  pinMode(S4, OUTPUT);
  pinMode(S5, OUTPUT);
  pinMode(S6, OUTPUT);
```

```
  pinMode(S7, OUTPUT);
  pinMode(S8, OUTPUT);
  Serial.begin(115200);

  while (!Serial) {
      // will pause Zero, Leonardo, etc until serial console opens
      delay(1);
  }



  // Initialize the INA219.
  // By default the initialization will use the largest range (32V, 2A).  However
  // you can call a setCalibration function to change this range (see comments).
  if (! ina219.begin()) {
    Serial.println("Failed to find INA219 chip");
    while (1) { delay(10); }
  }
  // To use a slightly lower 32V, 1A range (higher precision on amps):
  //ina219.setCalibration_32V_1A();
  // Or to use a lower 16V, 400mA range (higher precision on volts and amps):
  //ina219.setCalibration_16V_400mA();

  Serial.println("Measuring current and voltage");

}
void monitoring_system(){


  //Measuring Voltage
  voltageSensorVal = analogRead(voltageSensorPins[0]);    // read the current sensor value (0 - 1023)
  vOut = (voltageSensorVal / 1023) * vCC;             // convert the value to the real voltage on the analog pin
  vIn[0] =  vOut * factor;                              // convert the voltage on the source by multiplying with the factor
  Serial.print("Sensor ");
  Serial.print(1);
```

```
  Serial.print(" - Voltage = ");
  Serial.print(vIn[0], 3); // print with 3 decimals
  Serial.println("V");

  voltageSensorVal = analogRead(voltageSensorPins[1]);    // read the current sensor value (0 - 1023)
  vOut = (voltageSensorVal / 1023) * vCC;             // convert the value to the real voltage on the analog pin
  vIn[1] =  vOut * factor;                               // convert the voltage on the source by multiplying with the factor
  Serial.print("Sensor ");
  Serial.print(2);
  Serial.print(" - Voltage = ");
  Serial.print(vIn[1] - vIn[0], 3); // print with 3 decimals
  Serial.println("V");

  voltageSensorVal = analogRead(voltageSensorPins[2]);    // read the current sensor value (0 - 1023)
  vOut = (voltageSensorVal / 1023) * vCC;             // convert the value to the real voltage on the analog pin
  vIn[2] =  vOut * factor;                               // convert the voltage on the source by multiplying with the factor

  Serial.print("Sensor ");
  Serial.print(3);
  Serial.print(" - Voltage = ");
  Serial.print(vIn[2] - vIn[1], 3); // print with 3 decimals
  Serial.println("V");

  voltageSensorVal = analogRead(voltageSensorPins[3]);    // read the current sensor value (0 - 1023)
  vOut = (voltageSensorVal / 1023) * vCC;             // convert the value to the real voltage on the analog pin
  vIn[3] =  vOut * factor;                               // convert the voltage on the source by multiplying with the factor

  Serial.print("Sensor ");
  Serial.print(4);
  Serial.print(" - Voltage = ");
  Serial.print(vIn[3] - vIn[2], 3); // print with 3 decimals
  Serial.println("V");

  Serial.print("Overall Voltage = ");
  Serial.print(vIn[3],3);
```

```
  Serial.println("V");

  //Measure Current

  float current_A = 0;
  current_A = ina219.getCurrent_mA()/1000;
  Serial.print("Current: "); Serial.print(current_A, 3); Serial.println(" A");

  //Measure temperature
  for (int i = 0; i < 3; i++) {
    Vo = analogRead(ThermistorPins[i]);
    R2 = R1 * (1023.0 / (float)Vo - 1.0);
    logR2 = log(R2);
    T = (1.0 / (c1 + c2*logR2 + c3*logR2*logR2*logR2));
    T = T - 273.15;

    Serial.print("Temperature of batt ");
    Serial.print(i + 1);
    Serial.print(": ");
    Serial.print(T);
    Serial.println(" celcius");
    }
}

void loop() {

  monitoring_system();


  //Balancer control logic
  //Charge or Discharge upper batteries
  digitalWrite(S1, HIGH);
  digitalWrite(S2, LOW);
  digitalWrite(S3, HIGH);
  digitalWrite(S4, LOW);
```

```
  digitalWrite(S5, HIGH);
  digitalWrite(S6, LOW);
  digitalWrite(S7, HIGH);
  digitalWrite(S8, LOW);
  Serial.println("Upper Battery ");
  delay(10000);

  //Charge or Discharge lower batteries
  digitalWrite(S1, LOW);
  digitalWrite(S2, HIGH);
  digitalWrite(S3, LOW);
  digitalWrite(S4, HIGH);
  digitalWrite(S5, LOW);
  digitalWrite(S6, HIGH);
  digitalWrite(S7, LOW);
  digitalWrite(S8, HIGH);
  Serial.println("Lower Battery ");
  delay(10000);

}
```

Appendix B: Datasheet of LiFePo4 Battery 26650 3400mAh

IFR26650 3400mAh 3.2V LiFePo4 Battery	Low teerature 26650 battery cell Specification
Lithium Polymer Battery Manufacture	MaxPower Industrial Co.,Ltd
H.S. Code	850600090
Normal Capacity	3400mAh
Normal Voltage	3.2V
Energy	10.88wh
Dimension	26.3mm Height : 65.7mm
Internal Resistance	Less than 20mOhms
Charging Voltage	4.2V
Discharge Cut Off Voltage	3.0V
Charging Method	CC-CV(Constant voltage with limited current)
Weight	85g
Standard Charge current	0.5C
Standard discharge current	0.5C
Max. Charge current	3C
Max. discharge current	3C
battery protection function	over charge Protection ,over discharge protection ,teerature and balance function
Charge Teerature	-30-50 degree
Discharge teerature	-50-60 degree
Quality Guarantee	Five years
Application	AGV,Outdoor energy,Personnel tracking, cargo tracking ,power bank,tablet
	Solar System battery , EV ,EBIKE UPS,RV Caer ,military power

Appendix C: Datasheet of Voltage Sensor

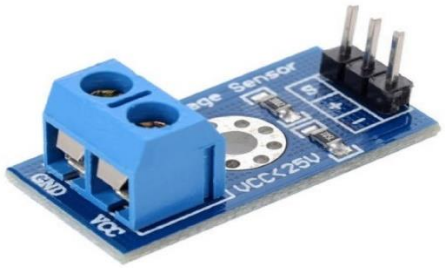

DESCRIPTION

A simple but very useful module which uses a potential divider to reduce any input voltage by a factor of 5.

This allows you to use the analogue input of a microcontroller to monitor voltages much higher than it capable of sensing.

For example with a 0-5V analogue input range you are able to measure a voltage up to 25V.

The module also includes convenient screw terminals for easy and secure connection of wires.

This module is based on principle of resistive voltage divider design, can make the red terminal connector input voltage to 5 times smaller

Arduino analog input voltages up to 5 v, the voltage detection module input voltage not greater than 5Vx5=25V (if using 3.3V systems, input voltage not greater than 3.3Vx5=16.5V).

Arduino AVR chips have 10-bit AD, so this module simulates a resolution of 0.00489V (5V/1023), so the minimum voltage of input voltage detection module is 0.00489Vx5=0.02445V.

- Input voltage : 25v DC max
- Divider ratio : 5:1
- Output voltage : 5v DC (input/5 input*0.2)
- Output Current : 600mA (MAX)
- Voltage detection range : DC0.02445V – 25V
- Voltage analog resolution : 0.00489 V
- Output Interface :
- “+ ” connected 5/3.3V
- “-” connected GND
- “s” connected Arduino AD pins
- Size : 25mm x 13mm / 0.98″ x 0.51″

Appendix D: Datasheet of INA219 Current Sensor

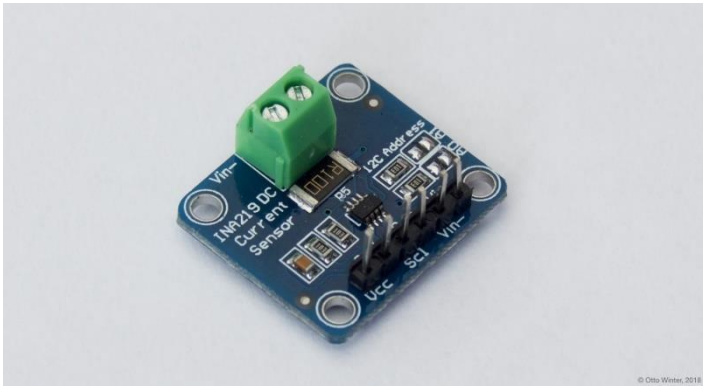

Features and Specifications

Operational Voltage: 3 – 5.5 Volts

Operating Temperature: -400C – 1250C

Maximum Voltage: 6 Volts

Bus Voltage Range: 0 – 26 Volts

Current sensing Range: ±3.2A with ±0.8mA resolution

0.1 ohm 1% 2W current sense resistor

Some of the extra features include: It has in-built calibration registers to reduce uncertainty in the power, voltage, and current values. It contains 16 programmable addresses and filtering options. The sensor is available in 2 grades i.e. INA219A and INA219B. The Accuracy is up to 0.5% in INA219B over the temperature. The sensor has two package types i.e. SOT23-8 and SOIC-8.